

**Figure 1 | Role of activated intestinal MCs in the development of intestinal inflammation.** (a) CD63 expression on colonic MCs was examined with flow cytometry. Cells were gated on c-kit<sup>+</sup> and FcεR1α<sup>+</sup> cells. (b) The percentage of CD63<sup>+</sup> MCs in all c-kit<sup>+</sup> FcεR1α<sup>+</sup> MCs was determined with flow cytometry at various time points after TNBS administration ( $n=3$  for day 6,  $n=5$  for day 3,  $n=7$  for intact, EtOH, day 1 and 2,  $n=14$  for day 4). Control mice were analysed 4 days after EtOH administration (EtOH;  $n=7$ ). Data are shown as means  $\pm$  s.e.m. (c) Colonic tissue sections from a healthy volunteer (HV) and UC and CD patients were stained with 4',6-diamidino-2-phenyl indole (blue) and MC tryptase (red) or haematoxylin and eosin (H&E) (bottom). Scale bars, 100  $\mu$ m. (d) Tryptase-positive MCs were counted in the fields of the tissue sections (four fields for each section). Data are means  $\pm$  s.e.m. ( $n=6$ ). (e) Body weight changes were monitored after TNBS administration to *Kit*<sup>W-sh/W-sh</sup> MC-deficient mice (*Kit*<sup>W-sh/W-sh</sup> EtOH; open triangles;  $n=4$ , *Kit*<sup>W-sh/W-sh</sup> TNBS; closed triangles;  $n=9$ ), *Kit*<sup>+/+</sup> control mice (*Kit*<sup>+/+</sup> EtOH; open diamonds;  $n=4$ , *Kit*<sup>+/+</sup> TNBS; closed diamonds;  $n=13$ ) and *Kit*<sup>W-sh/W+</sup> control mice (*Kit*<sup>W-sh/W+</sup> EtOH; open squares;  $n=4$ , *Kit*<sup>W-sh/W+</sup> TNBS; closed squares;  $n=11$ ). Data are shown as percentages of baseline weights and are means  $\pm$  s.e.m., \* $P<0.0001$  (two-tailed Student's *t*-test); \*\* $P=0.0024$  (two-tailed Student's *t*-test). (f) The colon was isolated 4 days after TNBS treatment for H&E staining. Data are representative of at least three independent experiments. Scale bars, 100  $\mu$ m. (g) Colon length was measured 4 days after colitis induction. EtOH, closed column; TNBS, open column. \* $P<0.0001$  (two-tailed Student's *t*-test), \*\* $P=0.0024$  (two-tailed Student's *t*-test). Data are shown as means  $\pm$  s.e.m. (h) The percentage of CD11b<sup>+</sup> Gr-1<sup>high</sup> cells in the colonic lamina propria was calculated, as measured with flow cytometry. EtOH, closed column; TNBS, open column. \* $P=0.0003$  (two-tailed Student's *t*-test), \*\* $P=0.0029$  (Welch's *t*-test) and \*\*\* $P<0.0001$  (Welch's *t*-test). Data are shown as means  $\pm$  s.e.m. (i) Colonic mononuclear cells were isolated 4 days after TNBS administration and stained with anti-CD11b and anti-Gr-1 antibodies. CD11b<sup>+</sup> Gr-1<sup>high</sup> cells were sorted and then stained with May-Giemsa stain. Scale bar, 20  $\mu$ m. Data are representative of three experiments.

the ATP-binding portion but lacking the C-terminal region) was detected by western blot, but its surface expression was not detected by flow cytometry because of its defect in extracellular expression (Supplementary Fig. S4d,e)<sup>24</sup>. In addition, neither western blot nor flow cytometry detected variant d (lacking the ATP-binding portion; Supplementary Fig. S4d,e). These data strongly suggest that 1F11 mAb recognizes P2X7 receptors, specifically the ATP-binding portion. We also confirmed that 1F11 mAb had similar reactivity to that of a commercially available anti-P2X7 mAb (clone: Hano43; Supplementary Fig. S4f,g).

To evaluate whether 1F11 mAb directly affects MCs during ATP-mediated activation, we treated MCs with ATP in the presence of 1F11 mAb *in vitro*. 1F11 mAb treatment reduced the number of CD63<sup>+</sup>-activated MCs induced by ATP in a dose-dependent manner (Fig. 4a). High concentrations of extracellular ATP increased the

cell permeability of the MCs<sup>12</sup>. Thus, uptake of Lucifer yellow was observed in ATP-stimulated MCs but was substantially impaired in 1F11 mAb-treated and *P2x7*<sup>-/-</sup> MCs (Fig. 4b,c).

As many cell types (MCs, T cells and DCs) express P2X7 receptors (Fig. 3b), we then asked whether the P2X7 receptors on MCs were responsible for the MC-mediated intestinal inflammation *in vivo* by analysing MC-deficient *Kit*<sup>W-sh/W-sh</sup> mice reconstituted with *P2x7*<sup>+/+</sup> or *P2x7*<sup>-/-</sup> MCs. We confirmed that reconstituted MCs were present in the colon and maintained P2X7 expression (Supplementary Fig. S5). Like wild-type mice, *Kit*<sup>W-sh/W-sh</sup> mice reconstituted with *P2x7*<sup>+/+</sup> MCs showed severe inflammatory responses when treated with TNBS. However, these inflammatory responses were ameliorated when *Kit*<sup>W-sh/W-sh</sup> mice were reconstituted with *P2x7*<sup>-/-</sup> MCs; the amelioration included inhibition of neutrophil infiltration and MC activation (Figs 1 and 5a–f).

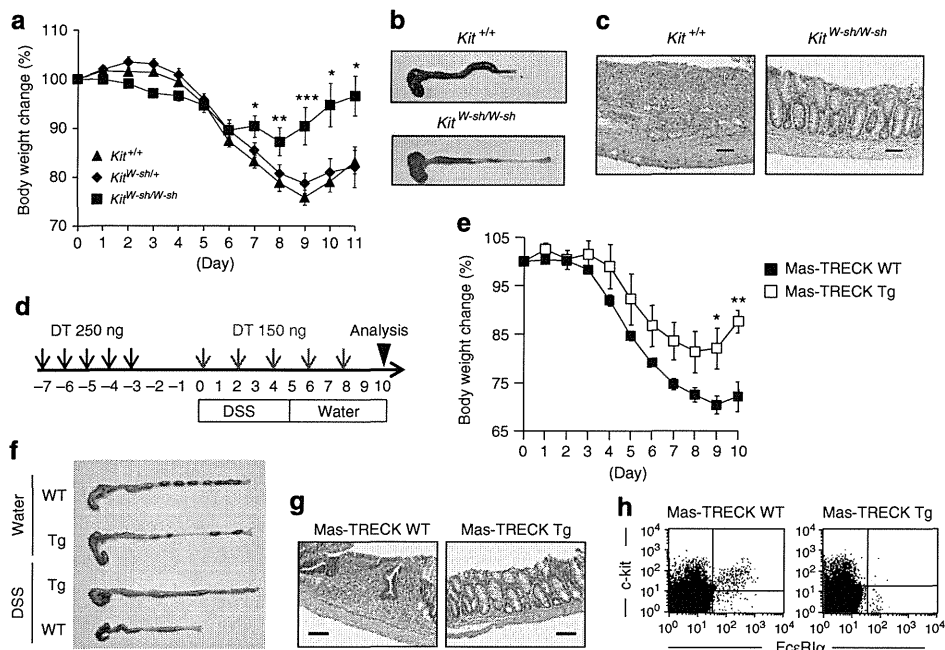


**Figure 2 | Impaired DSS-induced colitis in MC-deficient mice.** *Kit<sup>W-sh/W-sh</sup>* MC-deficient, *Kit<sup>+/+</sup>* control mice and Mas-TRECK transgenic (Tg) mice were subjected to DSS-induced colitis. **(a)** Body weight changes are shown as percentages of the baseline value and are means  $\pm$  s.e.m. ( $n = 22$  for *Kit<sup>+/+</sup>*;  $n = 25$  for *Kit<sup>W-sh/+</sup>*;  $n = 10$  for *Kit<sup>W-sh/W-sh</sup>*).  $*P < 0.01$ ,  $**P = 0.0207$  and  $***P = 0.0004$  (two-tailed Student's *t*-test). **(b,c)** Eleven days after DSS treatment, colon tissue and haematoxylin and eosin (H&E)-stained tissue sections were examined. Data are representative of at least three independent experiments. **(d)** Mas-TRECK Tg mice and their wild-type (WT) littermates were subjected to DSS-induced colitis. For diphtheria toxin (DT) treatment, mice were injected intraperitoneally with 250 ng of DT for 5 consecutive days (black arrows) and then with 150 ng every other day (red allows). **(e)** Body weight changes are shown as percentages of the baseline value and are means  $\pm$  s.e.m. ( $n = 6$  for Tg;  $n = 10$  for WT),  $*P = 0.0107$ ,  $**P = 0.0037$  (two-tailed Student's *t*-test). **(f)** Representative images of whole colons 10 days after DSS treatment. **(g)** Representative images of H&E staining. Scale bars, 100  $\mu$ m. **(h)** Representative flow cytometric data of infiltrated c-kit<sup>+</sup> Fc $\epsilon$ R1 $\alpha$ <sup>+</sup> MCs in the colon.

We next analysed whether the MCs in UC or CD patients expressed P2X7. Although increased number of MCs were observed in the colons of both UC and CD patients (Fig. 1c,d), P2X7 purinoceptors were expressed by the MCs in CD patients but not by those in UC patients or healthy volunteers (Fig. 5g,h). Thus, it is likely that P2X7 purinoceptor-mediated MC activation also occurs in the human colon, especially in CD patients.

To examine whether ATP was extracellularly released at high concentrations at inflammatory sites, we next measured ATP release from inflammatory colonic tissues. An elevated level of ATP release from the colon tissue was noted in TNBS-treated mice (Fig. 6a). In addition, intrarectal administration of non-hydrolyzable ATP (adenosine 5'-O-(3-thio) triphosphate and O-(4-benzoyl)benzoyl adenosine 5'-triphosphate) led to MC activation in the colonic tissue, similar to the effect of TNBS treatment (Fig. 6b). In contrast, intrarectal administration of other P2Y receptor agonists did not increase colonic MC activation (Fig. 6b). These findings indicate that inflammatory stimuli induce the extracellular release of ATP, which in turn leads to P2X7-dependent MC activation in the colon and subsequent exacerbation of intestinal inflammation.

P2X7 signalling activates the caspase-1 inflammasome to induce the production of IL-1 $\beta$  and IL-18 (ref. 25). IL-1 $\beta$  production is also mediated by MC proteases, such as chymases<sup>26</sup>. We therefore examined whether MCs produced IL-1 $\beta$  via P2X7 receptor activation, and if so whether this production was caspase-1-dependent. IL-1 $\beta$  production was decreased when P2X7-deficient MCs were stimulated with ATP, whereas substantial amounts of IL-1 $\beta$  were produced in caspase-1-deficient MCs (Supplementary Fig. S6), indicating that IL-1 $\beta$  production was P2X7-dependent but caspase-1-independent. In line with this finding, body weight changes were noted in *Kit<sup>W-sh/W-sh</sup>* mice reconstituted with *caspase-1<sup>-/-</sup>*

MCs (Fig. 5a). These results suggest that MC-dependent inflammation through P2X7 purinoceptors is not dependent on caspase-1-mediated IL-1 $\beta$  or IL-18 production.

**An autocrine loop of ATP conversion mediates MC activation.** In addition to ATP, other nucleotides (for example, extracellular ADP) act as signals to induce inflammatory responses<sup>27</sup>. We confirmed that MCs are activated by high concentrations of ADP and ATP (Fig. 7a,b). Extracellular ATP is hydrolysed by ectonucleoside triphosphate diphosphohydrolases (CD39) to ADP and AMP; it is then further hydrolysed by ecto-5'-nucleotidase (CD73) to adenosine, which has anti-inflammatory functions<sup>27</sup>. Colonic MCs expressed CD39 but not CD73 (Supplementary Fig. S7a,b), indicating that MCs can convert ATP to ADP but not to adenosine. We therefore examined the involvement of ADP-reactive P2Y purinoceptors and found that P2Y1 and P2Y12 were highly expressed on colonic MCs (Fig. 7c). However, inhibitors of P2Y1 and P2Y12 receptors, as well as knockdown of the P2Y12 receptor, had no effect on the induction of CD63<sup>+</sup>-activated MCs (Fig. 7d,e; Supplementary Fig. S8a). Similarly, intestinal inflammation, as well as activation of colonic MCs, was unaffected in clopidogrel (a P2Y12 receptor inhibitor)-treated mice (Supplementary Fig. S8b–d). These data indicate that although P2Y1 and P2Y12 were expressed on MCs neither P2Y1 nor P2Y12 purinoceptors mediate ADP-dependent CD63<sup>+</sup> MC induction.

It is generally accepted that P2X7 purinoceptors specifically recognize ATP<sup>7</sup>, but we found that they were also involved in ADP-mediated MC activation. Indeed, no activation was noted in *P2x7<sup>-/-</sup>* MCs when they were stimulated with ADP (Fig. 7f), leading us to hypothesize that ADP promotes ATP release from MCs and their subsequent stimulation. To test this hypothesis, we measured the expression of pannexin-1, connexin 43 and connexin 32, which

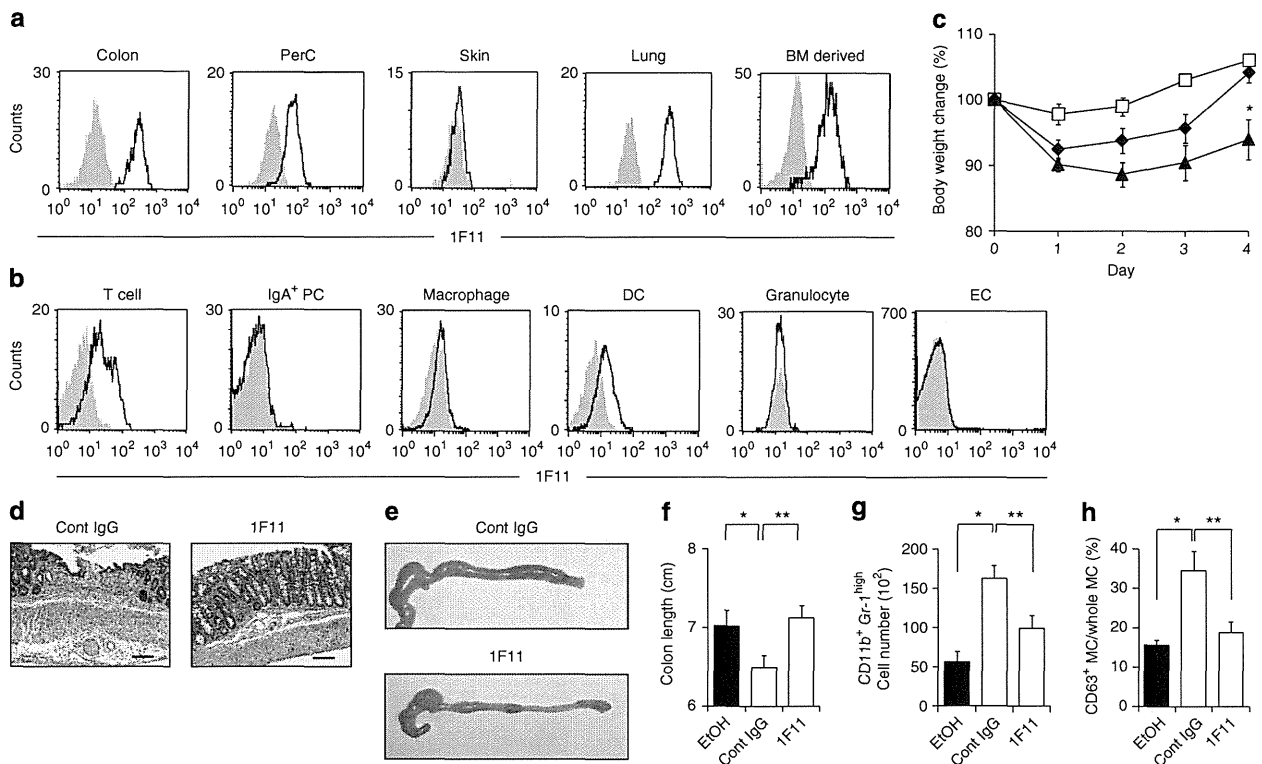


**Figure 3 | Amelioration of colitis by treatment with intestinal MC-reactive 1F11 mAb. (a)** MCs in the colonic lamina propria, peritoneal cavity (PerC), skin and lung, as well as BM-derived MCs, were stained with 1F11 mAb. Control staining with rat IgG2b is shown in grey. **(b)** Cells were isolated from colonic lamina propria and epithelium. CD3<sup>+</sup> T cells, IgA<sup>+</sup> plasma cells (PCs), F4/80<sup>+</sup> macrophages, CD11c<sup>+</sup> DCs, Gr1<sup>+</sup> granulocytes and ECs were gated and their reactivity to 1F11 mAb examined. Control staining with rat IgG2b is shown in grey. **(c)** C57BL/6 mice were treated with TNBS and their body weights were monitored for 4 days; 0.5 mg of 1F11 or the control mAb was intraperitoneally administered. Data from 9 (EtOH; open squares), 19 (TNBS with control mAb; closed triangles) and 12 (TNBS with 1F11 mAb; closed diamonds) mice. \**P* = 0.0066 (Welch's *t*-test). Data are shown as percentages of baseline weights and are means ± s.e.m. **(d,e)** Representative images of haematoxylin and eosin staining and colon tissue from 1F11 mAb-treated mice. Scale bars, 100 μm. **(f)** Colon length was measured 4 days after TNBS administration. \**P* = 0.0445; \*\**P* = 0.0073 (two-tailed Student's *t*-test). **(g)** Neutrophils (CD11b<sup>+</sup> Gr-1<sup>high</sup>) were quantified as percentages and numbers of cells. Data are shown as means ± s.e.m. (*n* = 6), \**P* < 0.0001, \*\**P* = 0.0047 (two-tailed Student's *t*-test). **(h)** Percentage of CD63<sup>+</sup> MCs in all c-kit<sup>+</sup> FcεR1α<sup>+</sup> MCs was determined with flow cytometry. Data are shown as means ± s.e.m. (*n* = 6) \**P* = 0.0202; \*\**P* = 0.0284 (two-tailed Student's *t*-test).

are ATP-releasing hemichannels, during cell activation<sup>28,29</sup>. The hemichannels were rarely expressed on the colonic MCs (Fig. 7g), and no inhibitory effect was observed when the MCs were treated with ADP in the presence of hemichannel inhibitors (flufenamic acid and carbenoxolone). However, cell activation was inhibited by P2X7 antagonists [oxidized ATP (OxATP), pyridoxal-phosphate-6-azophenyl-2',4'-disulfonate and 4,4'-diisothiocyanatostilbene-2,2'-disulfonic acid disodium salt hydrate] (Fig. 7h). To further exclude the possibility that ADP triggers ATP release, we stimulated MCs with another P2Y ligand (UTP); we found that UTP did not induce MC activation (Fig. 7b).

We then tested whether ADP was converted to ATP by ATP-converting enzymes such as ecto-adenylate kinase, ATP synthase and nucleoside diphosphokinase<sup>30</sup>. To test the involvement of these enzymes, we used inhibitors of ecto-adenylate kinase (diadenosine pentaphosphate; AD2P5), ATP synthase (oligomycin; oligo) and nucleoside diphosphokinase (UDP), and we found that inhibition of ecto-adenylate kinase and ATP synthase, but not nucleoside diphosphokinase, reduced ADP- as well as ATP-dependent MC activation (Fig. 7h,i). Neither AD2P5 nor oligo inhibited MC activation induced by the crosslinking of IgE with relevant allergen (Fig. 7i). Among the adenylylase kinases, adenylylase kinase 1 (AK1) and AK2 were expressed in colonic MCs, and the expression of AK2 was much higher than that of AK1 (Supplementary Fig. S9a). As with AD2P5 treatment, knockdown of AK2, but not AK1, led to the

inhibition of both ADP- and ATP-mediated MC activation (Supplementary Fig. S9b). These results indicate that P2X7 purinoceptors have an important role in the activation of MCs by ATP, including ATP derived from ADP by the action of ecto-enzymes such as ATP synthase and AK2.

**Neutrophil infiltration by MC-derived mediators.** Evaluation of MC activation on the basis of CD63 expression is an important criterion<sup>13</sup>; however, degranulation is not absolutely associated with cytokine production<sup>31</sup>. Therefore, we measured MC production of an array of inflammatory cytokine, chemokine and lipid mediators to additionally elucidate the role of P2X7 purinoceptor-mediated MC activation in the development of intestinal inflammation. Stimulation of MCs with ATP induced the production of inflammatory cytokines such as IL-6, tumour necrosis factor (TNF)α and oncostatin M<sup>32</sup>; this induction was not observed in *P2x7*<sup>-/-</sup> MCs or in wild-type MCs treated with 1F11 mAb (Fig. 8a,b).

We showed that neutrophil infiltration into the colon was mediated by MC activation (Fig. 1h,i), and a previous study suggested that neutrophil infiltration is a potential target in colitis treatment<sup>33</sup>. Consistent with these findings, ATP stimulation induced MCs, but not *P2x7*<sup>-/-</sup> MCs, to produce leukotrienes (LTs; LT C4/D4/E4), which are associated with the translocation of 5-lipoxygenase (5-LO) into the nucleus—an important step for LT synthesis in MCs<sup>34</sup> (Fig. 8c,d). Also, chemokine gene array analysis demonstrated that

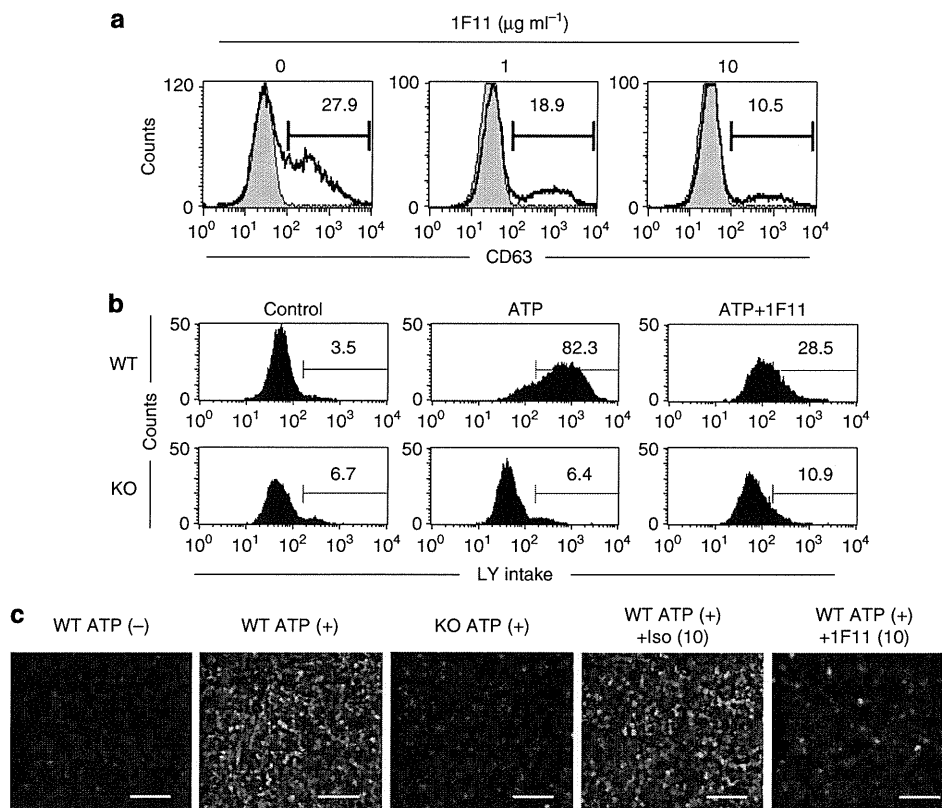


**Figure 4 | Inhibition of *in vitro* ATP-mediated MC activation by 1F11 mAb.** (a) BM-derived MCs, pretreated with various concentrations of 1F11 mAb (0, 1, 10  $\mu\text{g ml}^{-1}$ ) for 15 min, were stimulated with 0.5 mM ATP for 30 min. Cells were stained with an anti-CD63 mAb for flow cytometric analysis. Data are representative of three independent experiments. (b) BM-derived MCs pretreated with various concentrations of 1F11 mAb or control rat IgG2b (0, 10  $\mu\text{g ml}^{-1}$ ) for 15 min were stimulated with 0.5 mM ATP for 30 min in the presence of 1 mg  $\text{ml}^{-1}$  Lucifer yellow (LY). (c) LY uptake was determined by using flow cytometry and fluorescence microscopy. Scale bar, 100  $\mu\text{m}$ . Data are representative of three individual experiments.

ATP stimulation of MCs induced the expression of chemokines, including CCL2, CCL7 and CXCL2 (Fig. 8e–g), and 1F11 mAb treatment or P2X7 deficiency resulted in decreased CCL2 production from MCs activated by ATP but not by IgE plus allergen (Fig. 8g). Furthermore, *Kit<sup>W-sh/W-sh</sup>* mice showed decreased levels of both CCL2 and IL-1 $\beta$  in the colon tissue, but the production levels of these molecules recovered when the mice were reconstituted with wild-type MCs (Supplementary Fig. S10a). As neutrophils express the corresponding chemokine receptors, it is likely that ATP-dependent MC activation induced inflammatory neutrophil infiltration into the colon from the peripheral blood (Supplementary Fig. S10b,c), given the high level of TNF $\alpha$  production by the neutrophils (Supplementary Fig. S10d). These results indicate that ATP-dependent MC activation has key roles in the induction of inflammatory responses (by inducing inflammatory cytokines) and in the exacerbation of inflammatory responses (by inducing LTs and chemokines to recruit TNF $\alpha$ -producing neutrophils to the colon).

## Discussion

Here, we showed that MCs have a critical role in the severity of colitis through their interaction with ATP and P2X7 purinoceptors. These interactions not only induce MC-mediated inflammatory responses but also exacerbate them by promoting neutrophil infiltration. Indeed, MC-deficient mice reconstitution with wild-type, but not *P2x7<sup>-/-</sup>*, MCs resulted in neutrophil infiltration and severe inflammatory responses, together with increased production of IL-1 $\beta$ , LTs and CCL2 (Figs 5 and 8, and Supplementary Fig. S10). *Kit<sup>W-sh/W-sh</sup>* mice spontaneously show elevated levels of neutrophils in their spleens<sup>35</sup>; however, we confirmed that the neutrophil levels

were the same as those in the colons of *Kit<sup>+/+</sup>*, *Kit<sup>W-sh/+</sup>* and *Kit<sup>W-sh/W-sh</sup>* mice under naïve conditions (Fig. 1h,i). To exclude the possible involvement of other immunological defects in *Kit<sup>W-sh/W-sh</sup>* mice, such as the involvement of the *Corin* gene, which is associated with type II transmembrane serine protease<sup>35</sup>, we further confirmed the amelioration of intestinal inflammation in conditional MC-deficient mice (Fig. 2d–h). These findings strongly suggest that P2X7 on MCs has a pivotal role in the development of murine and human intestinal inflammation.

P2X7 purinoceptors are expressed on T cells, DCs, macrophages and ECs<sup>9–11,25,36</sup>. In a recent study, ATP/P2X7-mediated signalling inhibited the generation and function of regulatory T cells and ATP stimulation led to their conversion into Th17 cells via an IL-6-dependent pathway; thus, the P2X7 antagonist OxATP inhibited colitis<sup>37</sup>. In that study, ATP/P2X7-mediated regulation of regulatory T cells was involved in the chronic phase of intestinal inflammation, which takes about 4 weeks for disease development<sup>37</sup>. Similarly, ATP-mediated DC activation occurs in the chronic phase of intestinal inflammation through the preferential induction of Th17 cells, although whether this is mediated by P2X7 remains to be seen<sup>38</sup>. In contrast, ATP/P2X7-mediated MC activation in our model was important in the development of T-cell-independent acute colitis, which occurs within 1 week. Thus, our study and those of others<sup>37,38</sup> complement each other by reflecting the complicated pathological aspects and kinetics of the acute and chronic phases of intestinal inflammation mediated by ATP and P2X7.

We also found that the expression level of P2X7 receptors differed depending on the tissue and animal species. First, colonic MCs expressed high levels of P2X7, but skin MCs did not

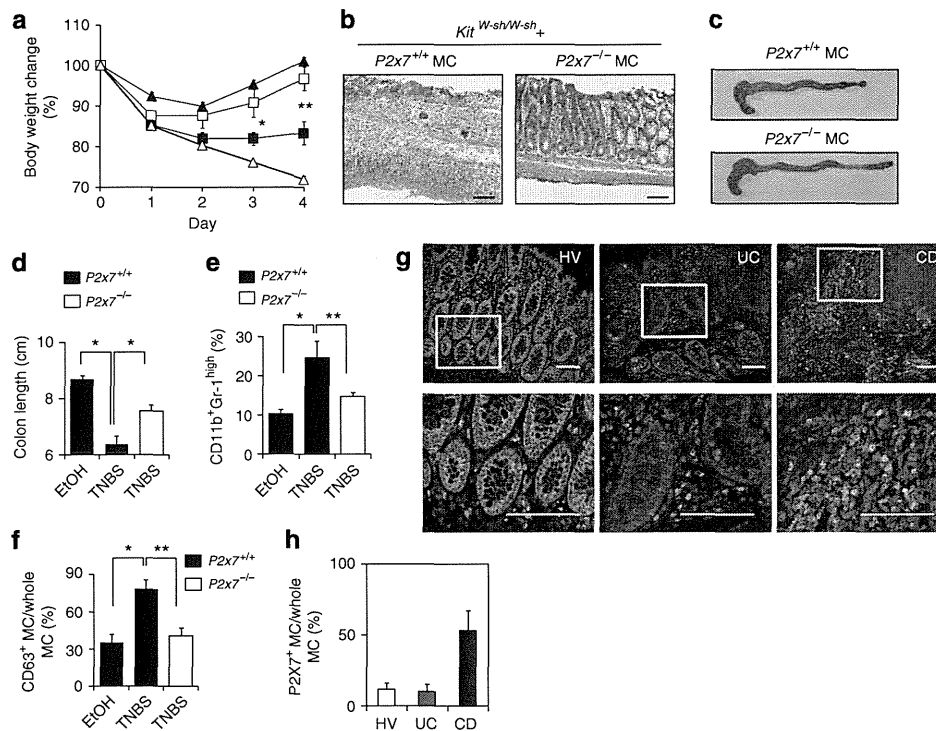


**Figure 5 | Inhibitory targeting of P2X7 purinoceptors on MCs leads to amelioration of colonic inflammation.** *Kit<sup>W-sh/W-sh</sup>* MC-deficient mice reconstituted with *P2x7<sup>+/+</sup>*, *P2x7<sup>-/-</sup>* or *caspase-1<sup>-/-</sup>* BM-derived MCs were applied to a TNBS-induced colitis model. **(a)** Body weight changes were monitored in TNBS-treated *Kit<sup>W-sh/W-sh</sup>* mice reconstituted with *P2x7<sup>+/+</sup>* (closed squares;  $n=9$ ), *P2x7<sup>-/-</sup>* (open squares;  $n=7$ ) or *caspase-1<sup>-/-</sup>* (open triangles;  $n=4$ ). BM-derived MCs were used for TNBS treatment, and *P2x7<sup>+/+</sup>* BM-derived MC-reconstituted *Kit<sup>W-sh/W-sh</sup>* mice receiving EtOH served as controls (closed triangles;  $n=3$ ).  $*P=0.0264$  (two-tailed Student's *t*-test),  $**P=0.0058$  (two-tailed Student's *t*-test). Data are shown as percentages of baseline weights and are means  $\pm$  s.e.m. **(b)** Representative images of haematoxylin and eosin staining are shown. Scale bars represent 100  $\mu$ m. **(c)** Representative images of whole colons are shown. **(d)** Colon length was measured 4 days after TNBS administration. Data are shown as means  $\pm$  s.e.m. ( $n=3$  for *P2x7<sup>+/+</sup>* EtOH,  $n=9$  for *P2x7<sup>+/+</sup>* TNBS,  $n=7$  for *P2x7<sup>-/-</sup>* TNBS),  $*P<0.001$  (two-tailed Student's *t*-test). **(e)** Representative flow cytometric data of infiltrated neutrophils (CD11b<sup>+</sup>Gr-1<sup>high</sup>) in the colon from three individual experiments.  $*P=0.00741$ ,  $**P=0.0009$  (two-tailed Student's *t*-test). Data are shown as means  $\pm$  s.e.m. **(f)** The percentage of CD63<sup>+</sup> MCs in all c-kit<sup>+</sup> FcεR1α<sup>+</sup> MCs was determined with flow cytometry. Data are shown as means  $\pm$  s.e.m. ( $n=3-9$ ),  $*P=0.007$  (Welch's *t*-test),  $**P=0.0234$  (Welch's *t*-test). **(g)** Colonic tissue sections from a healthy volunteer (HV) and from UC and CD patients were stained with 4',6-diamidino-2-phenyl indole (blue), MC tryptase (red) and P2X7 (green). Scale bars, 100  $\mu$ m. **(h)** Cells expressing both P2X7 and MC tryptase were counted in the fields of the tissue sections (four fields for each section). Data are means  $\pm$  s.e.m. ( $n=6$ ).

(Fig. 3a). Second, in contrast to MCs, some macrophages (for example, microglia and RAW264.7 cells) expressed higher levels of P2X7 than did colonic macrophages (Fig. 3b and data not shown). Third, among the several types of immunocompetent cell in the colon, MCs expressed the highest levels of P2X7 (Fig. 3a,b). Fourth, we found P2X7 expression on human colonic ECs, but not on murine colonic ECs (Figs 3b and 5g). In addition, as reported previously<sup>36</sup>, P2X7 expression on ECs was downregulated in the colons of CD patients; instead, CD patients showed increased numbers of P2X7<sup>+</sup> MCs in their colons (Fig. 5g,h). It is important to note that, like murine MCs, human lung MCs express functional P2X7 (ref. 39). Therefore, although we must recognize the similarities and differences between mouse and human intestinal inflammation and MC distribution, ATP/P2X7-mediated MC activation seems to have a major role in the development of intestinal inflammation.

We found elevated levels of extracellular ATP in the colons of TNBS-treated mice (Fig. 6a). This high ATP concentration was most likely achieved by a combination or cascade of several ATP production pathways (for example, cell injury or lysis<sup>7</sup>, pattern recognition receptor-mediated activation of monocytes<sup>40</sup> and commensal bacteria<sup>38</sup>). In our tissue culture system, we detected elevated release of ATP (40  $\mu$ M) in the inflamed colon compared with the control (Fig. 6); however, at least 100  $\mu$ M ATP was required for MC activation

*in vitro* in the single cell culture system (Fig. 7b). This disparity likely reflects the differences in the culture conditions. Unlike in the single cell culture system, the concentration of secreted ATP in the tissue culture system could have been diluted in the culture medium, or ATP could have been consumed rapidly by activated inflammatory cells in the tissue. Alternatively, a lack of commensal bacteria-derived ATP in the tissue culture system as a result of the inclusion of antibiotics may have reduced the ATP level. Another possibility is that the abundant endogenous ATP-degrading enzymes (for example, CD39) in the colon tissue may have degraded some of the ATP. In support of this idea, a suppressive role for CD39 in intestinal inflammation has been reported<sup>41</sup>.

We found that ADP-reactive P2Y1 and P2Y12 receptors were expressed on colonic MCs (Fig. 7c), but inhibition or knockdown of these receptors did not suppress the CD63 expression (Fig. 7d,e; Supplementary Fig. S8a). In previous studies, stimulation of MCs with ADP (0.05–50  $\mu$ M) has led to calcium influx via the P2Y1- but not the P2Y12-mediated pathway<sup>42</sup>, whereas our results indicate that CD63 expression required a higher concentration of ADP and was not suppressed by a P2Y1 inhibitor (Fig. 7b,d). This finding indicates that P2Y purinoceptors are not involved in the induction of CD63<sup>+</sup>-activated MCs that is mediated by high concentrations of ADP. However, we found that adenylate kinase and ATP synthase converted ADP back to ATP, which subsequently induced P2X7

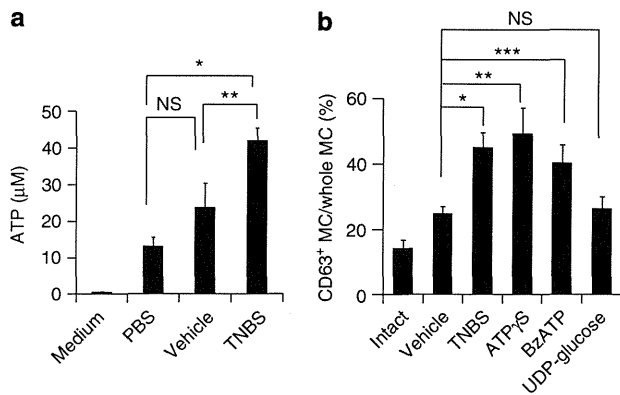


**Figure 6 | Enhanced ATP production in intestinal inflammation and MC activation induced by non-hydrolyzable ATP.**

(a) The concentration of ATP released from the colon tissue of mice receiving intrarectally administered phosphate-buffered saline, vehicle or TNBS was measured. Data are shown as means  $\pm$  s.e.m. ( $n=3-7$ ). \* $P=0.0004$ , \*\* $P=0.0447$  (two-tailed Student's  $t$ -test). (b) CD63 expression of colonic MCs was measured with flow cytometry after intrarectal administration of vehicle ( $n=14$ ), TNBS ( $n=5$ ), non-hydrolyzable ATP (adenosine 5'-O-(3-thio) triphosphate (ATP $\gamma$ S);  $n=9$  or O-(4-benzoyl)benzoyl adenosine 5'-triphosphate (BzATP);  $n=10$ ) or UDP-glucose ( $n=6$ ), or in intact mice ( $n=7$ ). Data are shown as means  $\pm$  s.e.m. \* $P=0.0002$  (two-tailed Student's  $t$ -test), \*\* $P=0.0135$  (Welch's  $t$ -test) and \*\*\* $P=0.0238$  (Welch's  $t$ -test). NS, not significant.

purinoceptor-dependent MC activation. A similar conversion of ADP to ATP has been reported for endothelial cells<sup>27</sup>. Among adenylate kinases, AK2 was highly expressed on MCs and had a pivotal role in the conversion of ADP to ATP (Supplementary Fig. S9a,b). As another P2Y ligand (UTP) did not induce MC activation (Fig. 7b), our findings suggest that ADP could be converted into ATP by AK2 and ATP synthase, and that this ATP subsequently activates MCs through P2X7 purinoceptors. In addition, colonic MCs do not express ecto-5'-nucleotidase (CD73), an enzyme that degrades ADP into adenosine, which has anti-inflammatory effects in intestinal inflammation<sup>43</sup>. Therefore, our study indicates that MCs express CD39, adenylate kinases and ATP synthase, but not CD73, to preferentially convert ADP to ATP for the exacerbation of inflammatory responses through P2X7 purinoceptors.

Here, we showed that colitis aggravated by P2X7-mediated activation of MCs was independent of the inflammasome pathway, and that P2X7-mediated activation of MCs promoted TNF $\alpha$  production by effector cells to further promote intestinal inflammation<sup>44</sup>. Our findings also suggest that MCs exacerbate inflammation by recruiting neutrophils to produce abundant TNF $\alpha$ , but less IL-10 than is produced by other cells (for example, eosinophils, DCs and macrophages; Supplementary Fig. S10d). This neutrophil recruitment was mediated by the production of IL-1 $\beta$ , LTs and chemokines, which are potential targets for the treatment of colitis. Mice with experimentally induced colitis that lack CXCR2 or 5-LO (a key enzyme for converting arachidonic acid to LTs), as well as mice treated with inhibitors of CCR2, CXCR2 or 5-LO, show reduced inflammation and less neutrophil recruitment in their colons<sup>33,45,46</sup>. Moreover, given that ATP promotes neutrophil migration<sup>47</sup>, it is possible that P2X7-dependent LT and chemokine production, as well as ATP generation via AK2 and ATP synthase from MCs, could amplify neutrophil infiltration of the colon. These data collectively indicate that MCs are key factors in the induction of intestinal inflammation and also recruit neutrophils to heighten inflammatory responses. P2X7-dependent MC activation could, therefore, be a target for the treatment of intestinal inflammation.

## Methods

**Mice and human samples.** Female C57BL/6 mice were purchased from CLEA Japan. Rag1<sup>-/-</sup> and P2x7<sup>-/-</sup> mice were obtained from Jackson Laboratory (Bar Harbor, ME, USA). MC-deficient *Kit*<sup>W-sh/W-sh</sup> mice were obtained from Dr H. Suto (Atopy Research Center, Juntendo University, Japan). For the conditional MC-deficient analysis, Mas-TRECK tg mice were injected intraperitoneally with 250 ng of diphtheria toxin for 5 consecutive days and then with 150 ng every other day<sup>18</sup>. *Caspase-1*<sup>-/-</sup> mice were backcrossed with C57BL/6 mice; F5 mice were used for this experiment<sup>48</sup>. All mice were maintained under specific-pathogen-free conditions at the Experimental Animal Facility of the Institute of Medical Science, the University of Tokyo. All experiments were approved by the Animal Care and Use Committee of the University of Tokyo.

MC reconstitution was performed as described previously<sup>49</sup>. Briefly, BM-derived MCs were obtained from P2x7<sup>+/+</sup>, P2x7<sup>-/-</sup> or *caspase-1*<sup>-/-</sup> mice as described previously<sup>22</sup>. BM-derived MCs ( $5 \times 10^6$ ) were intravenously transferred to *Kit*<sup>W-sh/W-sh</sup> mice at two time points (0 and 14 days). The reconstituted mice were used 3 months after the last transfer.

Colon specimens from UC and CD patients and healthy volunteers were obtained by endoscopic biopsy at Osaka University Hospital. All subjects provided written informed consent, and the study protocol was approved by the Ethics Committee of Osaka University Graduate School of Medicine (no. 08243) and the Institute of Medical Science, The University of Tokyo (no. 20-67-0331).

**Experimental colitis.** For TNBS-induced colitis, anaesthetized mice (18–22 g) were sensitized with 2.5% TNBS (Sigma-Aldrich) together with acetone and olive oil<sup>50</sup>. After 1 week, after a 3-h fast, the mice were given 100  $\mu$ l of 2.5% TNBS in 50% ethanol via a flexible feeding tube that maintained their heads in a vertical position for 10 min. The control group received only 50% ethanol. Weight changes were recorded daily, and tissues were collected for histological analysis and isolation of mononuclear cells from the colonic lamina propria. For mAb treatment, mice were injected intraperitoneally with 0.5 mg of mAb (1F11 or an isotype control) 1 day before being given TNBS/EtOH intrarectally. mAb administration was continued for 3 days. For P2Y12 inhibition with clopidogrel sulphate, (Wako, Osaka, Japan), mice received clopidogrel (0.5 mg ml<sup>-1</sup>) in their drinking water from 3 days before intrarectal administration of TNBS/EtOH until the end of the study<sup>50</sup>. For DSS-induced colitis, mice were given 3.5% DSS (Wako, for C57BL/6) or 2.5% DSS (MP Biomedicals, Illkirch, France, for Mas-TRECK tg mice) in their drinking water for 5 days and their body weights were monitored daily<sup>50</sup>. In some experiments, non-hydrolyzable ATP (adenosine 5'-O-(3-thio) triphosphate and O-(4-benzoyl)benzoyl adenosine 5'-triphosphate) or UDP-glucose (0.25 mg in 50% EtOH) was intrarectally administered and the effects were analysed 2 days later.

**In vitro MC stimulation and inhibition.** BM-derived MCs ( $2.5 \times 10^5$ ) were cultured with various concentrations of adenosine, ADP, ATP, UTP or anti-DNP-IgE with DNP-human serum albumin. Adenosine-3-phosphate 5-phosphosulfate (0.25 mM), carbenoxolone (10  $\mu$ M), flufenamic acid (100  $\mu$ M), pyridoxal-phosphate-6-azophenyl-2',4'-disulfonate (100  $\mu$ M), 4,4'-diisothiocyanatostilbene-2,2'-disulfonic acid disodium salt hydrate (100  $\mu$ M), OxATP (0.5 mM), AD2P5 (1 mM), oligo (10 or 100  $\mu$ M) or UDP (100  $\mu$ M) was added to the cells for the inhibition assay<sup>27,28,40,51</sup>. All reagents were purchased from Sigma-Aldrich (St Louis, MO, USA, purity was  $\geq 95\%$ ). 5-LO (BD Pharmingen, Franklin Lakes, NJ, USA) was stained after permeabilization with 0.2% Triton-X100 for 10 min; nuclei were stained with 4',6-diamidino-2-phenyl indole.

**Cell preparation and flow cytometry.** ECs and lamina propria mononuclear cells were isolated from the colon, as described previously<sup>52</sup>. For flow cytometric analysis, cells were incubated with 5  $\mu$ g ml<sup>-1</sup> of an anti-CD16/32 antibody (10  $\mu$ g ml<sup>-1</sup>, Fc block, BD Pharmingen) for 5 min and stained for 30 min at 4  $^{\circ}$ C with fluorescence-labeled Abs specific for c-kit (0.2  $\mu$ g ml<sup>-1</sup>), Gr-1 (0.4  $\mu$ g ml<sup>-1</sup>), CD4 (1  $\mu$ g ml<sup>-1</sup>), CD11b (0.2  $\mu$ g ml<sup>-1</sup>), CD11c (0.4  $\mu$ g ml<sup>-1</sup>), CD39 (0.4  $\mu$ g ml<sup>-1</sup>), CD45 (0.4  $\mu$ g ml<sup>-1</sup>), IgA (10  $\mu$ g ml<sup>-1</sup>), B220 (0.4  $\mu$ g ml<sup>-1</sup>, BD Pharmingen), CCR3 (2  $\mu$ g ml<sup>-1</sup>), CXCR2 (4  $\mu$ g ml<sup>-1</sup>, R&D Systems, Minneapolis, MN, USA), Fc $\epsilon$ RI $\alpha$  (0.4  $\mu$ g ml<sup>-1</sup>), CD73 (0.4  $\mu$ g ml<sup>-1</sup>), TLR2 (10  $\mu$ g ml<sup>-1</sup>; eBioscience, San Diego, CA, USA), F4/80 (20  $\mu$ g ml<sup>-1</sup>), CCR2 (10  $\mu$ g ml<sup>-1</sup>), P2X7 (Hano43; 2  $\mu$ g ml<sup>-1</sup>, Serotec, UK) or CCR1 (10  $\mu$ g ml<sup>-1</sup>, Abnova, Taiwan). Flow cytometric analysis and cell sorting were performed by using FACSCalibur and FACSAria (BD Biosciences, Franklin Lakes, NJ, USA), respectively. Sorted cells were stained with May-Giemsa stain in some experiments. Colonic MCs and BM-derived MCs were prepared as described elsewhere<sup>22</sup>.

**Establishment of an anti-P2X7 mAb (1F11) and an anti-CD63 mAb.** The procedure used to establish MC-specific mAbs is shown as a flowchart in Supplementary Figure S3. Briefly, c-kit<sup>+</sup> Fc $\epsilon$ RI $\alpha$ <sup>+</sup> MCs were obtained as described previously<sup>22</sup> from the colons of mice that exhibited allergic diarrhoea. Purified colonic MCs ( $10^6$  cells) were injected into the footpads of Sprague Dawley rats seven times, as described previously<sup>53</sup>. Lymphocytes were isolated from the spleen and inguinal lymph nodes and fused with P3X63-AG8.653 myeloma cells (CRL-1580; American Type Culture Collection, Manassas, VA, USA). The reactivity of each hybridoma to the colonic MCs was examined by means of flow cytometry. To identify antigens



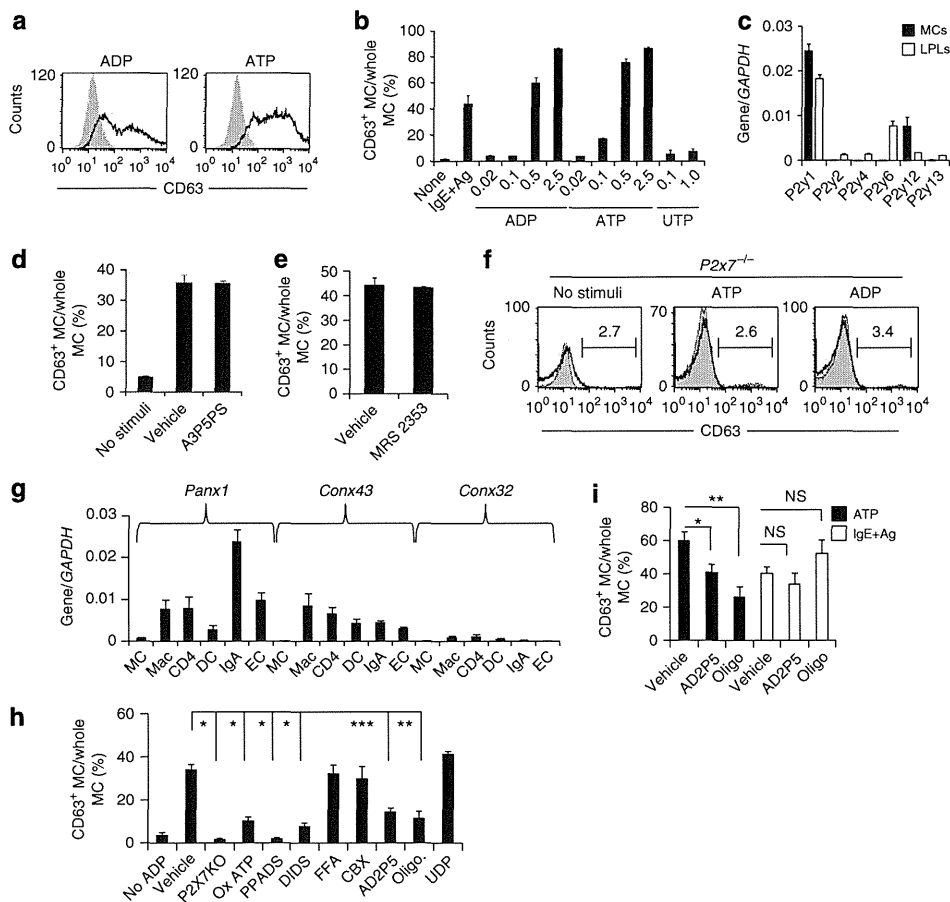


**Figure 7 | The ecto-adenylate kinase pathway mediates ADP-dependent MC activation through P2X7 purinoceptors.** (a) BM-derived MCs treated with ADP or ATP at 0.5 mM for 30 min and examined for CD63 expression. (b) BM-derived MCs treated with IgE plus relevant allergen or various concentrations of ADP, ATP or UTP for the analysis of CD63 expression. Data are representative of four experiments. (c) Expression of mRNA encoding each P2Y receptor in colonic lamina propria lymphocytes (LPLs) and MCs was analysed by quantitative reverse transcription (RT)-PCR ( $n = 3$ ). (d,e) BM-derived MCs pre-treated with 0.25 mM P2Y1 inhibitor (adenosine-3-phosphate 5-phosphosulfate (A3P5PS)) (d) or 0.01 mM P2Y12 inhibitor (MRS2353) (e), stimulated with ADP and examined for CD63 expression ( $n = 3$ ). (f) BM-derived MCs from  $P2x7^{-/-}$  mice stimulated with ATP or ADP; CD63 expression was determined with flow cytometry. Data are representative of four experiments. (g) Expression of pannexin-1 (Panx1), connexin-43 (Conx43) and Connx32 on colonic MCs, macrophages (Mac), CD4<sup>+</sup> T cells (CD4), DCs, IgA<sup>+</sup> cells (IgA) and ECs was measured by quantitative RT-PCR ( $n = 4$ ). (h) BM-derived MCs were pretreated with inhibitors of P2X receptors [OxATP, 0.5 mM; pyridoxal-phosphate-6-azophenyl-2',4'-disulfonate (PPADS); 4,4'-diisothiocyanatostilbene-2,2'-disulfonic acid (DIDS)], connexins [flufenamic acid (FFA)], Panx-1 [carbenoxolone (CBX)], ecto-adenylate kinase [diadenosine pentaphosphate (AD2P5)], ATP synthase (oligomycin) or nucleoside diphosphokinase (UDP) and subsequently stimulated with 0.25 mM ADP. CD63 expression was determined with flow cytometry. ( $n = 3$ ) \* $P < 0.01$ , \*\* $P < 0.05$  (two-tailed Student's *t*-test). All data are shown as means  $\pm$  s.e.m. (i) BM-derived MCs were treated with AD2P5, oligomycin or UDP and stimulated with 0.5 mM ATP or IgE plus allergen. CD63 expression was determined with flow cytometry ( $n = 5$ ). \* $P < 0.0001$  (two-tailed Student's *t*-test), \*\* $P = 0.0008$  (two-tailed Student's *t*-test) and \*\*\* $P = 0.0008$  (Welch's *t*-test). NS, not significant.

recognized by the mAbs, immunoprecipitation was performed with the mAbs, followed by Liquid chromatography–mass spectrometry analysis, as described previously<sup>53</sup>. Antigen specificity was confirmed by transfecting CHO cells with plasmids that encoded the murine P2X7 receptor and CD63.

#### Measurements of membrane permeability and inflammatory mediators.

To assess membrane permeability, BM-derived MCs were washed twice with phosphate-buffered saline (PBS) and incubated with 1 mg ml<sup>-1</sup> Lucifer yellow (Sigma-Aldrich) containing 250  $\mu$ M sulfapyrazone (Sigma-Aldrich). The MCs were then stimulated with 0.5 mM ATP (Sigma-Aldrich) for 15 min, as described elsewhere<sup>12</sup>. In the inhibition assay, 1 or 10  $\mu$ g ml<sup>-1</sup> of 1F11 mAb or the control antibody (Rat IgG2b) was added before ATP stimulation. The fluorescence signal of Lucifer yellow was determined by using fluorescence microscopy (BZ9000, Keyence, Osaka, Japan) and flow cytometry.

To measure the production of cytokines, chemokines and LTs from MCs, BM-derived MCs ( $2.5 \times 10^5$ ) were stimulated with 2.5 mM ATP for 30 min, after which the supernatants were collected. Chemokine and cytokine production was detected with an inflammatory cytokine kit (BD Pharmingen). For IL-1 $\beta$  measurement, BM-derived MCs from wild-type,  $P2x7^{-/-}$  and  $caspace-1^{-/-}$  mice

were stimulated with 0.1  $\mu$ g ml<sup>-1</sup> of LPS for 4 h, followed by ADP or ATP stimulation. LT C4/D4/E4 production was detected by use of an enzyme-linked immunosorbent assay (GE Healthcare Bio-Science, NJ, USA). For ATP, cytokine and chemokine measurements from the colon tissue, the colon tissues were isolated from mice 2 days after intrarectal administration of TNBS. Released ATP was measured by culturing colon tissues at 100 mg of tissue per 100  $\mu$ l of RPMI1640 medium for 3 h and using a luminescence ATP detection system (PerkinElmer, Norwalk, CT, USA).

**Immunoprecipitation and western blotting.** Cell lysates obtained from BM-derived MCs or CHO transfectants (mouse P2X7 variants a, c and d and flag-mP2X7s, cloned from C57BL/6 mice) were analysed by western blotting and immunoprecipitation with 1F11 mAb or the control Ab. Membranes were probed with an anti-flag and a polyclonal rabbit anti-P2X7 antibody (Sigma-Aldrich).

**Histology.** Colonic tissues were fixed in 4% paraformaldehyde and embedded in paraffin. Tissue sections (5  $\mu$ m) were stained with haematoxylin and eosin solution, as described previously<sup>22</sup>. For the detection of MCs and P2X7

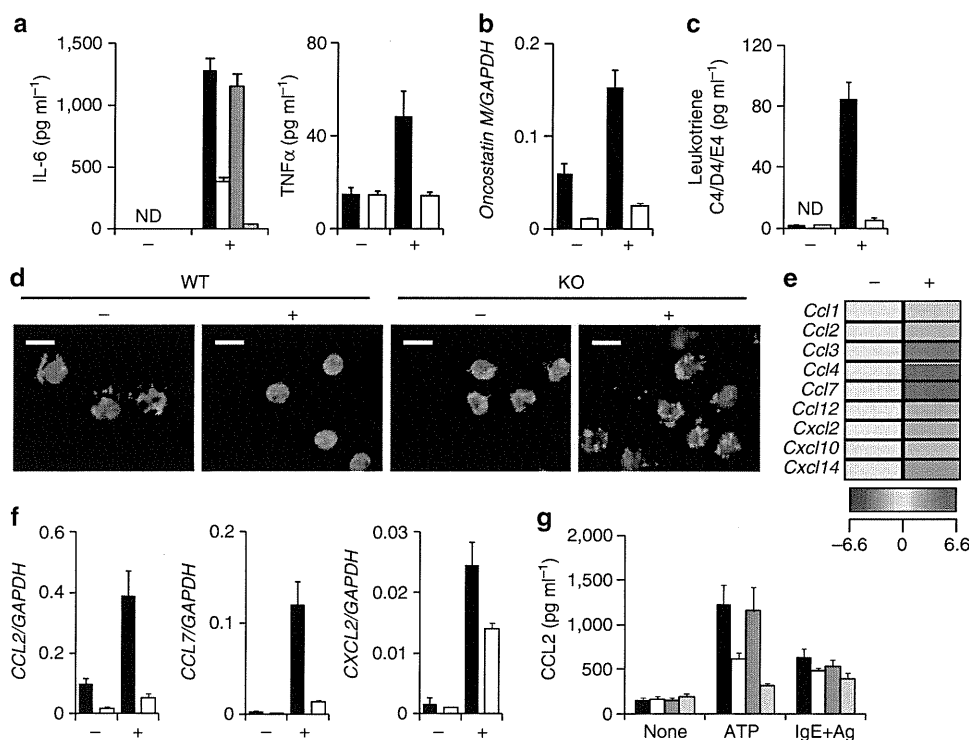


**Figure 8 | Critical role of the intestinal MC-associated ATP-P2X7 purinoceptor pathway for induction of neutrophil infiltration.**  $P2x7^{+/+}$  and  $P2x7^{-/-}$  BM-derived MCs were treated with 0.25 mM ATP (+) or left untreated (-). **(a)** Production of IL-6 (left panel; isotype mAb-treated MC, closed column; 1F11 mAb-treated MC, open column;  $P2x7^{+/+}$ , grey column; and  $P2x7^{-/-}$ , beige column) and TNF $\alpha$  (right panel) in culture supernatant ( $P2x7^{+/+}$ , closed column;  $P2x7^{-/-}$ , open column) was determined after 24 h stimulation. ND, not detected. Data are shown as means  $\pm$  s.e.m. ( $n=3$ ). **(b)** Oncostatin M mRNA expression was measured 30 min after stimulation of  $P2x7^{+/+}$  (closed column) and  $P2x7^{-/-}$  (open column) MCs with ATP. Data are shown as means  $\pm$  s.e.m. ( $n=3$ ). **(c)** LT C4/D4/E4 production from ATP-stimulated (+) or -unstimulated (-)  $P2x7^{+/+}$  (closed column) or  $P2x7^{-/-}$  BM-derived MCs (open column) in culture supernatants was measured by using enzyme-linked immunosorbent assay (ELISA). Data are shown as means  $\pm$  s.e.m. ( $n=3$ ). ND, not detected. **(d)**  $P2x7^{+/+}$  and  $P2x7^{-/-}$  BM-derived MCs were stimulated with 0.5 mM ATP. Cells were fixed and stained with an anti-5LO antibody (red) and 4',6-diamidino-2-phenyl indole (blue). Scale bar, 10  $\mu$ m. Data are representative of two experiments. **(e)** Representative data of a chemokine gene array are shown. Increased levels of each chemokine are shown as a heat map. **(f)** mRNA expression of CCL2 (left), CCL7 (middle) and CXCL2 (right) was measured by using quantitative reverse transcription-PCR. Data are shown as means  $\pm$  s.e.m. ( $n=3$ ). **(g)** CCL2 production was enumerated by using ELISA 24 h after stimulation of BM-derived MCs with ATP or IgE plus antigen (IgE + Ag). Isotype mAb-treated MC, closed column; 1F11 mAb-treated MC, open column;  $P2x7^{+/+}$  MC, grey column; and  $P2x7^{-/-}$  MC, beige column). Data are shown as means  $\pm$  s.e.m. ( $n=3$ ).

expression in human specimens, colonic tissue sections were stained with antibodies for MC tryptase and P2X7 purinoceptors (Alomone Laboratories, Jerusalem, Israel).

**shRNA plasmid construction and lentiviral transduction.** For the construction of shRNA expression lentivirus vector plasmids, a series of oligonucleotide pairs were synthesized, as listed below. Each oligo pair was annealed and cloned into pmU6<sup>54</sup>. Each mU6-shRNA cassette was then subcloned into the  $\Delta$ U3 sequence of the 3'-LTR of the lentivirus vector plasmid pLGC to generate pLGC-shCD63 (sense: 5'-TTTGATTCTTGCTGCATCAACATAGCTTCTGCTCACTATGTTGATGCGCAGCAAGAATCTTTTGG-3', antisense: 5'-AATTCAAAAAAGATTCTTGCTGCAACAACATAGTGACAGGAAGCTATGTTGATGCGCAGCAAGAAT-3'), pLGC-shP2Y12 (sense: 5'-TTTGATCTACTAATGATTCTAACTGCTTCCGTGTCACAGTTAGAATCATTAGTAGATCTTTTGG-3', antisense: 5'-AATTCAAAAAAGATCTACTAA TGATTCTAACTGTCACAGGAAGCAGTTAGAATCATTAGTAGAT-3') and pLGC-shAK1 (sense: 5'-TTTGGGAGAAAGATTGTACAGAAATGCTTCTGTCACATTTCTGTACAATCTTCTCGCTTTTGG-3', antisense: 5'-AATTCAAAAA GCGAGAAGATTGTACAGAAATGTGACAGGAAGCATTCTGTACAATCTTCTCG-3') and pLGC-shAK2 (sense: 5'-TTTGGGAGCTAATTGAGAAGAATTGC TTCTGTGCAAAATCTTCTCAATTAGCTCCATTTTGG-3', antisense: 5'-AATTCAAAAAATGGAGCTAATTGAGAAGAATTGTGACAGGAAGCA ATTTCTCAATTAGCTCC-3').

To obtain lentivirus-encoding green fluorescent protein (as a reporter gene) and shRNA for CD63, 293FT cells ( $6 \times 10^5$ ) were transfected with pLP1, pLP2, pLP-VSVG and pLGC-shRNA by using Lipofectamine 2000 (Invitrogen, Carlsbad, CA, USA) as per the manufacturer's protocol (Invitrogen). After 24- and 48-h incubations, lentivirus-encoding shRNA was collected.

BM-derived MCs ( $1 \times 10^6$ ) or MC/9 cells were transduced with shRNA expression lentivirus stock in the presence of  $8 \mu\text{g ml}^{-1}$  Polybrene (Sigma-Aldrich)<sup>55</sup>.

After 24 h, the cells were washed and green fluorescent protein-positive cells were sorted by FACSaria and used for subsequent experiments.

**Quantitative real-time-PCR.** Total RNA was prepared by using TRIzol (Invitrogen) and reverse transcribed by use of Superscript VILO (Invitrogen), as described. Quantitative reverse transcription-PCR was performed with the LightCycler 480 II (Roche, Mannheim, Germany) and the Universal Probe Library (Roche). Primer sequences are listed in Supplementary Table S1.

**Statistical analysis.** Statistical analysis was performed by using the unpaired two-tailed Student's *t*-test and Welch's *t*-test. The data are presented as means  $\pm$  s.e.m.

## References

1. Abraham, C. & Cho, J. H. Inflammatory bowel disease. *N Engl. J. Med.* **361**, 2066–2078 (2009).
2. Strober, W. & Fuss, I. J. Proinflammatory cytokines in the pathogenesis of inflammatory bowel diseases. *Gastroenterology* **140**, 1756–1767 (2011).
3. Alvarez-Errico, D., Lessmann, E. & Rivera, J. Adapters in the organization of mast cell signaling. *Immunol. Rev.* **232**, 195–217 (2009).
4. Bischoff, S. C. Role of mast cells in allergic and non-allergic immune responses: comparison of human and murine data. *Nat. Rev. Immunol.* **7**, 93–104 (2007).
5. Galli, S. J., Borregaard, N. & Wynn, T. A. Phenotypic and functional plasticity of cells of innate immunity: macrophages, mast cells and neutrophils. *Nat. Immunol.* **12**, 1035–1044 (2011).
6. He, S. H. Key role of mast cells and their major secretory products in inflammatory bowel disease. *World J. Gastroenterol.* **10**, 309–318 (2004).
7. Surprenant, A. & North, R. A. Signaling at purinergic P2X receptors. *Annu. Rev. Physiol.* **71**, 333–359 (2009).



8. Erlinge, D. P2Y receptors in health and disease. *Adv. Pharmacol.* **61**, 417–439 (2011).
9. Wilhelm, K. *et al.* Graft-versus-host disease is enhanced by extracellular ATP activating P2X7R. *Nat. Med.* **16**, 1434–1438 (2010).
10. Weber, F. C. *et al.* Lack of the purinergic receptor P2X(7) results in resistance to contact hypersensitivity. *J. Exp. Med.* **207**, 2609–2619 (2010).
11. Muller, T. *et al.* A potential role for P2X7R in allergic airway inflammation in mice and humans. *Am. J. Respir. Cell Mol. Biol.* **44**, 456–464 (2011).
12. Sudo, N. *et al.* Extracellular ATP activates mast cells via a mechanism that is different from the activation induced by the cross-linking of Fc receptors. *J. Immunol.* **156**, 3970–3979 (1996).
13. Furuno, T., Teshima, R., Kitani, S., Sawada, J. & Nakanishi, M. Surface expression of CD63 antigen (AD1 antigen) in P815 mastocytoma cells by transfected IgE receptors. *Biochem. Biophys. Res. Commun.* **219**, 740–744 (1996).
14. Rijniere, A., Koster, A. S., Nijkamp, F. P. & Kraneveld, A. D. Critical role for mast cells in the pathogenesis of 2,4-dinitrobenzene-induced murine colonic hypersensitivity reaction. *J. Immunol.* **176**, 4375–4384 (2006).
15. Kaser, A., Zeissig, S. & Blumberg, R. S. Inflammatory bowel disease. *Annu. Rev. Immunol.* **28**, 573–621 (2010).
16. Feyerabend, T. B. *et al.* Cre-mediated cell ablation contests mast cell contribution in models of antibody- and T cell-mediated autoimmunity. *Immunity* **35**, 832–844 (2011).
17. Otsuka, A. *et al.* Requirement of interaction between mast cells and skin dendritic cells to establish contact hypersensitivity. *PLoS One* **6**, e25538 (2011).
18. Sawaguchi, M. *et al.* Role of mast cells and basophils in IgE responses and in allergic airway hyperresponsiveness. *J. Immunol.* **188**, 1809–1818 (2012).
19. Fiorucci, S. *et al.* Importance of innate immunity and collagen binding integrin  $\alpha 1\beta 1$  in TNBS-induced colitis. *Immunity* **17**, 769–780 (2002).
20. Yoshimoto, T. & Nakanishi, K. Roles of IL-18 in basophils and mast cells. *Allergol. Int.* **55**, 105–113 (2006).
21. Pastorelli, L. *et al.* Epithelial-derived IL-33 and its receptor ST2 are dysregulated in ulcerative colitis and in experimental Th1/Th2 driven enteritis. *Proc. Natl Acad. Sci. USA* **107**, 8017–8022 (2010).
22. Kurashima, Y. *et al.* Sphingosine 1-phosphate-mediated trafficking of pathogenic Th2 and mast cells for the control of food allergy. *J. Immunol.* **179**, 1577–1585 (2007).
23. Nicke, A. *et al.* A functional P2X7 splice variant with an alternative transmembrane domain 1 escapes gene inactivation in P2X7 knock-out mice. *J. Biol. Chem.* **284**, 25813–25822 (2009).
24. Smart, M. L. *et al.* P2X7 receptor cell surface expression and cytolitic pore formation are regulated by a distal C-terminal region. *J. Biol. Chem.* **278**, 8853–8860 (2003).
25. Di Virgilio, F. Liaisons dangereuses: P2X<sub>7</sub> and the inflammasome. *Trends Pharmacol. Sci.* **28**, 465–472 (2007).
26. Mizutani, H., Schechter, N., Lazarus, G., Black, R. A. & Kupper, T. S. Rapid and specific conversion of precursor interleukin 1 $\beta$  (IL-1 $\beta$ ) to an active IL-1 species by human mast cell chymase. *J. Exp. Med.* **174**, 821–825 (1991).
27. Yegutkin, G. G. Nucleotide- and nucleoside-converting ectoenzymes: important modulators of purinergic signalling cascade. *Biochim. Biophys. Acta.* **1783**, 673–694 (2008).
28. Locovei, S., Bao, L. & Dahl, G. Pannexin 1 in erythrocytes: function without a gap. *Proc. Natl Acad. Sci. USA* **103**, 7655–7659 (2006).
29. Kang, J. *et al.* Connexin 43 hemichannels are permeable to ATP. *J. Neurosci.* **28**, 4702–4711 (2008).
30. Burrell, H. E. *et al.* Human keratinocytes release ATP and utilize three mechanisms for nucleotide interconversion at the cell surface. *J. Biol. Chem.* **280**, 29667–29676 (2005).
31. Foger, N. *et al.* Differential regulation of mast cell degranulation versus cytokine secretion by the actin regulatory proteins Coronin1a and Coronin1b. *J. Exp. Med.* **208**, 1777–1787 (2011).
32. Salamon, P. *et al.* Human mast cells release oncostatin M on contact with activated T cells: possible biologic relevance. *J. Allergy Clin. Immunol.* **121**, 448–455 e5 (2008).
33. Bento, A. F. *et al.* The selective nonpeptide CXCR2 antagonist SB225002 ameliorates acute experimental colitis in mice. *J. Leukoc. Biol.* **84**, 1213–1221 (2008).
34. Luo, M., Jones, S. M., Peters-Golden, M. & Brock, T. G. Nuclear localization of 5-lipoxygenase as a determinant of leukotriene B<sub>4</sub> synthetic capacity. *Proc. Natl Acad. Sci. USA* **100**, 12165–12170 (2003).
35. Nigrovic, P. A. *et al.* Genetic inversion in mast cell-deficient *Wsh* mice interrupts corin and manifests as hematopoietic and cardiac aberrancy. *Am. J. Pathol.* **173**, 1693–1701 (2008).
36. Cesaro, A. *et al.* Amplification loop of the inflammatory process is induced by P2X7R activation in intestinal epithelial cells in response to neutrophil transepithelial migration. *Am. J. Physiol. Gastrointest Liver Physiol.* **299**, G32–G42 (2010).
37. Schenk, U. *et al.* ATP inhibits the generation and function of regulatory T cells through the activation of purinergic P2X receptors. *Sci. Signal* **4**, ra12 (2011).
38. Atarashi, K. *et al.* ATP drives lamina propria T<sub>H</sub>17 cell differentiation. *Nature* **455**, 808–812 (2008).
39. Wareham, K., Vial, C., Wykes, R. C., Bradding, P. & Seward, E. P. Functional evidence for the expression of P2X1, P2X4 and P2X7 receptors in human lung mast cells. *Br. J. Pharmacol.* **157**, 1215–1224 (2009).
40. Piccini, A. *et al.* ATP is released by monocytes stimulated with pathogen-sensing receptor ligands and induces IL-1 $\beta$  and IL-18 secretion in an autocrine way. *Proc. Natl Acad. Sci. USA* **105**, 8067–8072 (2008).
41. Friedman, D. J. *et al.* From the Cover: CD39 deletion exacerbates experimental murine colitis and human polymorphisms increase susceptibility to inflammatory bowel disease. *Proc. Natl Acad. Sci. USA* **106**, 16788–16793 (2009).
42. Feng, C., Mery, A. G., Beller, E. M., Favot, C. & Boyce, J. A. Adenine nucleotides inhibit cytokine generation by human mast cells through a Gs-coupled receptor. *J. Immunol.* **173**, 7539–7547 (2004).
43. Louis, N. A. *et al.* Control of IFN- $\alpha$ A by CD73: implications for mucosal inflammation. *J. Immunol.* **180**, 4246–4255 (2008).
44. Rijniere, A., Koster, A. S., Nijkamp, F. P. & Kraneveld, A. D. TNF- $\alpha$  is crucial for the development of mast cell-dependent colitis in mice. *Am. J. Physiol. Gastrointest. Liver Physiol.* **291**, G969–G976 (2006).
45. Cuzzocrea, S. *et al.* 5-Lipoxygenase modulates colitis through the regulation of adhesion molecule expression and neutrophil migration. *Lab. Invest.* **85**, 808–822 (2005).
46. Waddell, A. *et al.* Colonic eosinophilic inflammation in experimental colitis is mediated by Ly6C<sup>high</sup> CCR2<sup>+</sup> inflammatory monocyte/macrophage-derived CCL11. *J. Immunol.* **186**, 5993–6003 (2011).
47. Chen, Y. *et al.* Purinergic signaling: a fundamental mechanism in neutrophil activation. *Sci. Signal* **3**, ra45 (2010).
48. Kuida, K. *et al.* Altered cytokine export and apoptosis in mice deficient in interleukin-1 $\beta$  converting enzyme. *Science* **267**, 2000–2003 (1995).
49. Tsai, M., Grimaldeston, M. A., Yu, M., Tam, S. Y. & Galli, S. J. Using mast cell knock-in mice to analyze the roles of mast cells in allergic responses *in vivo*. *Chem. Immunol. Allergy* **87**, 179–197 (2005).
50. Wirtz, S., Neufert, C., Weigmann, B. & Neurath, M. F. Chemically induced mouse models of intestinal inflammation. *Nat. Protoc.* **2**, 541–546 (2007).
51. Ransford, G. A. *et al.* Pannexin 1 contributes to ATP release in airway epithelia. *Am. J. Respir. Cell Mol. Biol.* **41**, 525–534 (2009).
52. Kunisawa, J. *et al.* Sphingosine 1-phosphate dependence in the regulation of lymphocyte trafficking to the gut epithelium. *J. Exp. Med.* **204**, 2335–2348 (2007).
53. Nochi, T. *et al.* A novel M cell-specific carbohydrate-targeted mucosal vaccine effectively induces antigen-specific immune responses. *J. Exp. Med.* **204**, 2789–2796 (2007).
54. Yu, J. Y., DeRuiter, S. L. & Turner, D. L. RNA interference by expression of short-interfering RNAs and hairpin RNAs in mammalian cells. *Proc. Natl Acad. Sci. USA* **99**, 6047–6052 (2002).
55. Haraguchi, T., Ozaki, Y. & Iba, H. Vectors expressing efficient RNA decoys achieve the long-term suppression of specific microRNA activity in mammalian cells. *Nucleic Acids Res.* **37**, e43 (2009).

## Acknowledgements

We thank Drs T. Kitamura and J. Kitaura (The University of Tokyo) for discussions and for providing reagents; Dr H. Suto (Juntendo University) for providing *Kit<sup>W-sh/W-sh</sup>* mice; Dr S. Nakae (The University of Tokyo) for advice on analysing *Kit<sup>W-sh/W-sh</sup>* mice; Drs S. Ohmi, M. Oyama, H. Hata and C. Takamura (The University of Tokyo) for protein analysis; and Dr A. Uozumi, I. Ishikawa and M. Mejima (The University of Tokyo), Drs F. Ishikawa and Y. Saito (RCAI) for technical advice. This work was supported by grants from: the Ministry of Education, Science, Sports and Technology of Japan (Grant-in Aid for Scientific Research S (23229004 to H.K.), for Young Scientists A (22689015 to J.K.), for Scientific Research on Innovative Areas (23116506 to J.K.), for Scientific Research on Priority Areas (19059003 to H.K.), for Challenging Exploratory Research (24659217 to J.K.), Leading-edge Research Infrastructure Program (J.K. and H.K.); the Young Researcher Overseas Visits Program for Vitalizing Brain Circulation of the Japan Society for the Promotion of Science (JSPS; J.K., H.K., Y.K., T.N.), and for JSPS Fellows (021-07124 to Y.K.); the Ministry of Health and Welfare of Japan (J.K. and H.K.); the Global Center of Excellence Program of the Center of Education and Research for Advanced Genome-based Medicine (H.K.); the Program for Promotion of Basic and Applied Research for Innovations in Bio-oriented Industry (BRAIN to J.K.); and the Yakult Bio-Science Foundation (J.K.).

## Author contributions

Y.K. conducted the research, performed experiments and wrote the manuscript; T.A. and K.F. performed gene expression and animal experiments; T.N. conducted the mAb experiment; H.T., H. Iba, T.H., M.K. and S.S. contributed to the experimental design and data analysis; S.N. and H. Iijima obtained clinical samples and J.K. and H.K. supervised the project and wrote the manuscript. JK should be contacted for material requests.

**Additional information**

Supplementary Information accompanies this paper at <http://www.nature.com/naturecommunications>

Competing financial interests: The authors declare no competing financial interests.

Reprints and permission information is available online at <http://npg.nature.com/reprintsandpermissions/>

**How to cite this article:** Kurashima, Y. *et al.* Extracellular ATP mediates mast cell-dependent intestinal inflammation through P2X7 purinoceptors. *Nat. Commun.* 3:1034 doi: 10.1038/ncomms2023 (2012).

**License:** This work is licensed under a Creative Commons Attribution-NonCommercial-Share Alike 3.0 Unported License. To view a copy of this license, visit <http://creativecommons.org/licenses/by-nc-sa/3.0/>



## Multiple microRNAs induced by Cdx1 suppress Cdx2 in human colorectal tumour cells

Takanobu TAGAWA\*, Takeshi HARAGUCHI\*, Hiroaki HIRAMATSU\*, Kazuyoshi KOBAYASHI\*, Kouhei SAKURAI\*, Ken-Ichi INADA† and Hideo IBA\*<sup>1</sup>

\*Division of Host–Parasite Interaction, Department of Microbiology and Immunology, Institute of Medical Science, University of Tokyo, 4-6-1 Shirokanedai, Minato-ku Tokyo 108-8639, Japan, and †First Department of Pathology, Fujita Health University School of Medicine, Aichi, Japan

The mammalian transcriptional factors, Cdx1 and Cdx2 (Cdx is caudal-type homeobox) are paralogues and critical for the cellular differentiation of intestinal or colorectal epithelia. It has been reported previously that in *Cdx1* transgenic or knockout mice, endogenous Cdx2 levels are inversely correlated with Cdx1 levels. Recently, we found that exogenous Cdx1 expression can suppress Cdx2 in a human colorectal tumour cell line, SW480, although the underlying molecular mechanisms were unclear. In the present study, we show that several microRNAs induced by exogenous Cdx1 expression directly bind to the *CDX2* mRNA 3'UTR (untranslated region) to destabilize these transcripts, finally leading to their degradation. Using microarray analysis, we found that several miRNAs that were computationally predicted to target *CDX2* mRNAs are up-regulated by exogenous Cdx1

expression in SW480 cells. Among these molecules, we identified *miR-9*, *miR-16* and *miR-22* as having the potential to suppress Cdx2 through the binding of the 3'UTR to its transcript. Importantly, simultaneous mutations of both the *miR-9*- and *miR-16*-binding sites in the *CDX2* 3'UTR were shown to be sufficient to block Cdx2 suppression. The results of the present study suggest a unique feature of miRNAs in which they contribute to homeostasis by limiting the levels of transcription factors belonging to the same gene family.

**Key words:** caudal-type homeobox gene 1 (*CDX1*), caudal-type homeobox gene 2 (*CDX2*), *hsa-miR-9*, *hsa-miR-16*, *hsa-miR-22*, microRNA (miRNA).

### INTRODUCTION

*Cdx* (caudal-type homeobox) genes encode HOX domain-containing transcription factors that are conserved among vertebrates. In mouse and humans, these genes are expressed during development in a tissue-specific manner and contribute to the formation of the anterior–posterior axis. In adults, two paralogues, Cdx1 and Cdx2, are expressed in the intestinal epithelium, and aberrant expression is often associated with metaplasias or tumour formation [1,2]. These factors have in fact been shown to be expressed in intestinal metaplasias [3], which are lesions that can progress to gastric adenocarcinoma. These two paralogous proteins are expected to play, at least partially, similar roles in the regulation of target gene expression by binding to identical recognition sequences [4,5]. However, it has also been shown that there are several regulatory interactions between Cdx1 and Cdx2 [6,7], suggesting that these two homologous transcription factors are not always functionally redundant.

Previous observations in *Cdx1* transgenic mice and *Cdx1*<sup>-/-</sup> mice have indicated that altered Cdx1 levels cause an inverse and dose-dependent modification of endogenous Cdx2 protein expression in the distal colon and jejunum [8]. It has also been reported that the expression of endogenous Cdx2 protein and mRNA is drastically reduced by ectopic Cdx1 expression in the small intestinal villi and colon surface epithelium of mice [9]. These results suggest that Cdx1 fine-tunes the expression of the *Cdx2* gene. Importantly, we have shown that ectopic Cdx1 expression in the colon cancer cell line SW480 significantly reduces endogenous Cdx2 protein [10].

miRNAs (microRNAs) are a group of 19–25 bp small RNAs that function as gene repressors of a vast range of genes via

their direct binding to the 3'UTR (untranslated region) of the corresponding mRNAs in a sequence-specific manner [11,12]. Given that several layers of regulation are likely to underlie the suppression of Cdx2 by Cdx1, we speculated that miRNAs would be involved in some of these pathways as the 3'UTR sequences of the *CDX1* and *CDX2* transcripts are not homologous. miRNA binding is largely dependent upon a 7 bp 'seed' sequence which corresponds to the 2–8 nt from the 5'-end of each of these molecules [13]. Since miRNAs depend on relatively weak binding specificity, they can potentially regulate hundreds of genes simultaneously and, at the same time, a specific mRNA can be targeted by multiple miRNAs [13]. In the present study, we show using colon tumour cell lines that Cdx1 induces the expression of several miRNAs, some of which repress Cdx2 expression.

### EXPERIMENTAL

#### Cell culture, transduction of virus vectors and transfection of plasmids

Established human cell lines SW480 (colorectal tumour), T84 (colorectal tumour) and PLAT [HEK (human embryonic kidney)-293 cells carrying pGag-pol-IRES-bs<sup>r</sup>] were grown in DMEM (Dulbecco's modified Eagle's medium; Gibco) with 10% FBS (fetal bovine serum; Wako). SW480 or T84 cells were transduced with the VSV-G (vesicular stomatitis virus glycoprotein) pseudotype retrovirus vector pMXs-IP (empty vector) or pMXs-Cdx1-IP (Cdx1 vector) after concentration by centrifugation. For selection, the cells were then cultivated for 4–6 days in the presence of 4.0 µg/ml puromycin. SW480 cells

Abbreviations used: CDX/Cdx, caudal-type homeobox; GAPDH, glyceraldehyde-3-phosphate dehydrogenase; miRNA, microRNA; RT, reverse transcription; UTR, untranslated region; VSV-G, vesicular stomatitis virus glycoprotein.

<sup>1</sup> To whom correspondence should be addressed (email iba@ims.u-tokyo.ac.jp).

were transfected with plasmids using Lipofectamine™ 2000 (Invitrogen) following the manufacturer's protocols and then cultivated for an additional 48 h.

### Retroviral vector

PLAT cells ( $4 \times 10^6$ ) were co-transfected with 2.7  $\mu\text{g}$  of pCAG-VSV-G and 8  $\mu\text{g}$  of either pMXs-IP or pMXs-Cdx1-IP [10] using Lipofectamine™ 2000. Supernatants were collected at 24 and 48 h after transfection, mixed and kept as VSV-G pseudotype retrovirus stocks.

### Plasmid construction

Oligonucleotides listed in Supplementary Table S1 (at <http://www.BiochemJ.org/bj/447/bj4470449add.htm>) were used as primers for the PCR cloning of the 3'UTR of *CDX2* mRNA (NM\_001265.4) from the HCT116 genome. The amplified product was subcloned into the pGEM-T Easy vector (Promega) to generate pGEM-T Easy-Cdx2\_3'UTR. For the generation of luciferase reporter vectors with mutations at putative miRNA-binding sites, site-directed mutagenesis was performed using Pyrobest (TaKaRa Bio) and the oligonucleotides listed in Supplementary Table S1. Both wild-type and mutated vectors were then digested by NotI in the presence of alkaline phosphatase (TaKaRa Bio) and the resultant 3'UTR fragments were inserted into the NotI site of psiCHECK-2 (Promega) to generate the luciferase assay reporter vector psiCHECK-2-Cdx2\_3'UTR and mutated reporter vectors as shown in Figure 2, and Supplementary Figures S1 and S2 (at <http://www.BiochemJ.org/bj/447/bj4470449add.htm>). The oligonucleotides used as primers for mutagenesis were designed not to create unintended sequences which have Watson-Crick-type complementarity to the seed sequences (2–8 nt from the 5'-end) of any human microRNAs listed in miRBase Release 14 (<http://www.mirbase.org/>) [14].

The oligonucleotides listed in Supplementary Table S1 were also used as PCR primer pairs to synthesize DNA with pre-miRNA sequences acquired from miRBase Release 14. After digestion with BbsI and EcoRI, the amplicons were inserted into the BbsI/EcoRI site of pmU6 [15] to generate pmU6-miR9-3, pmU6-miR22-2, pmU6-miR107 and pmU6-miR181b-2 respectively. For *miR16-1*, the amplified DNA insert was subcloned into the pCR2.1 vector and digested with BbsI and EcoRI. The resultant fragment was then inserted into the BbsI/EcoRI site of pmU6 [15] to generate pmU6-miR16-1.

### Protein and RNA preparation

Total proteins were extracted from cells using SDS buffer [100 mM Tris/HCl (pH 6.8), 12% 2-mercaptoethanol, 20% glycerol and 2% SDS] and heating at 95°C for 10 min. Total RNAs were extracted using the mirVana miRNA Isolation kit (Applied Biosystems) in accordance with the manufacturer's instructions.

### Immunoblotting analysis

Protein samples were separated by SDS/PAGE (12 mA for 60 min, followed by 24 mA for 90 min) and transferred on to an Immobilon-P (Millipore) filter under 20% methanol/80% Tris-Glycine buffer [25 mM Tris and 192 mM glycine (pH 8.5)] for 1 h at 120 V. For blocking, the membrane was soaked with 5% (w/v) non-fat dried skimmed milk (Wako), 95% PBS (tubulin and

Cdx1) or TBST (Tris-buffered saline pH 7.4 with 0.05% Tween 20) (Cdx2), shaken for 60 min and then incubated with primary antibody diluted in 1% (w/v) non-fat dried skimmed milk in PBS (tubulin and Cdx1) or TBST (Cdx2) for 16 h at 4°C. After washing with PBS (tubulin and Cdx1) or TBST (Cdx2), the membrane was reacted with secondary antibody [donkey anti-rabbit HRP (horseradish peroxidase) conjugate (Millipore)] diluted to 1:3000 by 1% (w/v) non-fat dried skimmed milk in PBS (tubulin and Cdx1) or TBST (Cdx2), for 1 h at room temperature (22°C). After washing with PBS (tubulin and Cdx1) or TBST (Cdx2), signals were detected using an ECL (enhanced chemiluminescence) kit (GE Healthcare) or ImmunoStar™ kit (Wako). Detection and quantification was performed using a LAS-4000 UVmini imager (Fuji Film). The primary antibodies used and their dilution ratios were as follows: anti-tubulin (used at 1:10000, rabbit IgG; Abcam) and anti-Cdx2 (used at 1:100, rabbit IgG; Cell Signaling Technology). Rabbit polyclonal antibodies against human Cdx1 were raised against a synthetic peptide (CLATSSP-MPVKEEFLP) and the dilution ratio for immunoblotting was 1:200.

### Quantitative RT (reverse transcription)-PCR

The oligonucleotides listed in Supplementary Table S1 were used as primer pairs to assay *CDX2* and *GAPDH* (glyceraldehyde-3-phosphate dehydrogenase) mRNA by quantitative RT-PCR. The Prime Script RT-PCR kit (TaKaRa Bio) was used for RT, and SYBR Green PCR Master Mix (Applied Biosystems) and the ABI 7300 real-time PCR system (Applied Biosystems) were used for real-time PCR in accordance with the manufacturer's instructions. For miRNAs, the TaqMan miRNA RT Kit (Applied Biosystems) was used for RT and TaqMan Universal PCR Master Mix (Applied Biosystems) and the ABI 7300 real-time PCR system (Applied Biosystems) were used for real-time PCR and detection respectively, in accordance with the manufacturer's instructions. Student's *t* test analysis was performed for each analysis.

### Dual luciferase assay

SW480 cells ( $1 \times 10^5$  cells per well in a 24-well plate) or transduced SW480 cells ( $1 \times 10^4$  cells per well in a 24-well plate) were transfected with 50 ng of luciferase assay reporter vectors and analysed using the Dual-Luciferase Reporter Assay system (Promega) and Glo-max 96 Microplate Luminometer (Promega) to detect both firefly luciferase activity and *Renilla* luciferase activity. Firefly luciferase activity was used as an internal control to normalize the *Renilla* luciferase activity levels. Student's *t* test was performed for each analysis.

### Analysis of miRNAs by microarray

miRNA microarray Rel.12.0 (Agilent Technologies), a Spike-In kit (Agilent Technologies) and an Agilent DNA Scanner C type (Agilent Technologies) were used to analyse human miRNA expression profiles. For calibration and quantification, Feature Extraction software (Agilent Technologies) was used and probes with a detected raw signal <1.0 were excluded as background noise. As a result, 198 out of 851 human miRNAs listed in miRBase Reference 12 were detected either using the pMXs-IP data set or pMXs-Cdx1 data set. Values acquired from each probe were processed on Microsoft Excel and the signals of undetected probes were set to 1.0 as a logarithm scale was used for this analysis.

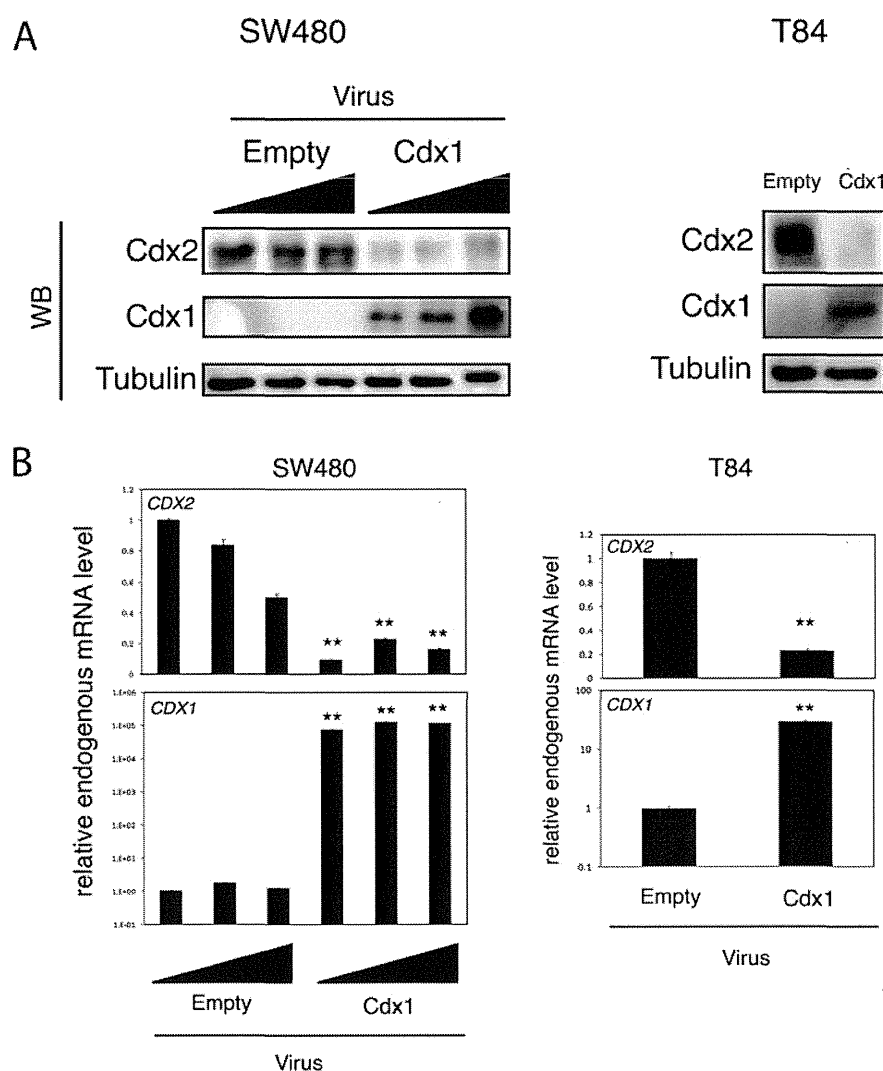


**Figure 1** Exogenous Cdx1 expression suppresses Cdx2 in the colorectal tumour cell lines SW480 and T84

SW480 or T84 cells were transduced either with VSV-G-type retroviral Cdx1 vector (pMXs-Cdx1-IP) or with empty vector and then selected by puromycin. At 6 days after transduction, total protein and RNA were prepared. In the case of transduction into SW480 cells, three viral dosages [MOI (multiplicity of infection) of 0.3, 1.0 and 3.0] were used. (A) Immunoblot analysis of Cdx2, Cdx1 and tubulin (loading control). (B) Quantitative RT-PCR analysis of *CDX2* and *CDX1*. Data are normalized using *GAPDH* and are shown as a relative value to the control of the empty vector transduction (MOI of 0.3). \*\* $P < 0.01$  compared with the mock-infected control. IP, immunoprecipitation; WB, Western blot.

## RESULTS

### Exogenously expressed Cdx1 suppresses both Cdx2 protein and mRNA expression in the SW480 and T84 colorectal tumour cell lines

We selected two colorectal cancer cell lines, SW480 and T84, to analyse the molecular mechanisms of Cdx2 suppression by Cdx1. This is because both SW480 and T84 express *CDX2* mRNA at high levels, and also because SW480 practically does not express *CDX1* and T84 expresses *CDX1* only marginally [10,16]. Consistent with our previous observation [10], SW480 cells transduced with a Cdx1 retrovirus vector at several doses showed a significant loss of Cdx2 protein when compared with those transduced with the empty vector (Figure 1A). Quantitative RT-PCR analysis further revealed that *CDX2* mRNA was also suppressed in these cells (Figure 1B).

Although it was previously reported that, in mice intestine or colon epithelium, exogenous expression of *Cdx1* decreases *Cdx2*

only when *Cdx1* expression surpasses a certain threshold [8,9], the results from our *in vitro* carcinoma cell line system suggest that Cdx1 transduction was so efficient that even the smallest dose was sufficient to maximally suppress Cdx2 (Figure 1).

A similar suppression of Cdx2 protein or *CDX2* mRNA by exogenous expression of Cdx1 was observed in the experiment using the T84 cell line (Figure 1).

### Various miRNAs are induced by exogenous Cdx1 expression, some of which were computationally predicted to target *CDX2* mRNA

We have hypothesized in the present study that Cdx1 fine-tunes the expression of the *CDX2* gene through specific miRNAs. Therefore we computationally predicted miRNAs that target *CDX2* mRNA using the algorithms PicTar (<http://pictar.mdc-berlin.de/>) and TargetScan (<http://www.targetscan.org/>), and identified 16 miRNAs that could putatively bind to the 3'UTR of *CDX2*

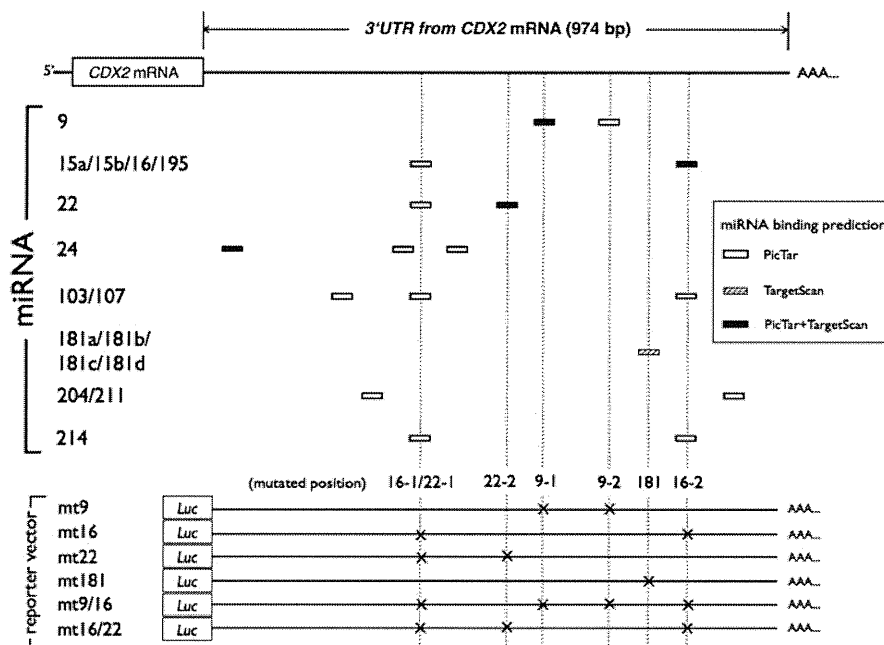


**Figure 2** miRNAs predicted to target the 3'UTR of the *CDX2* mRNA

miRNAs and their putative binding sites on the *CDX2* 3'UTR were predicted using PicTar or TargetScan (restricted to targets which are 'broadly conserved among vertebrates'). The first nucleotide position of each putative binding site is also indicated by its position relative to the 5'-end of the *CDX2* 3'UTR. Precise binding sequences predicted are provided in Supplementary Figure S3 (at <http://www.BiochemJ.org/bj/447/bj4470449add.htm>). CDS, coding sequence; *Luc*, luciferase.

mRNA (Figure 2 and Supplementary Figure S3 at <http://www.BiochemJ.org/bj/447/bj4470449add.htm>). Interestingly, only a marginal number of targets were predicted in the *CDX1* mRNA 3'UTR, although both *Cdx1* and *Cdx2* are paralogues that originated from the chicken *CdxA* gene. This suggested that *CDX1* and *CDX2* are regulated in a distinct manner, at least in terms of targeting by miRNAs. To investigate the possibility that miRNAs have important roles in *Cdx2* suppression, we first performed miRNA microarray analysis to detect the miRNAs that are induced by *Cdx1*. SW480 cells transduced with a *CDX1* retrovirus vector, which reduced the *Cdx2* protein levels (Figure 1A), were used for the microarray analysis. Nine out of 16 miRNAs predicted to target *Cdx2* were found to be up-regulated, whereas only two were found to be down-regulated when compared with mock-transduced SW480 cells (Table 1 and Figure 3). The remainder of the predicted miRNAs was not detectable in either the empty or *CDX1*-integrated samples. On the basis of these miRNA microarray results, we selected ten miRNAs (indicated by circles and rectangles in Figure 3) for further analysis by quantitative RT-PCR. Using the same RNA samples, we found a good correlation between the quantitative RT-PCR and microarray results (Table 1). *miR-9*, *miR-15a/miR-15b/miR-16*, *miR-22*, *miR-107* and *miR-181a/miR-181b* were then selected as the first panel of candidate miRNAs that are responsible for *Cdx2* suppression via *Cdx1* in tumour cells.

To further examine the activity of our candidate miRNA series, we constructed a reporter vector containing the 3'UTR of *CDX2* mRNA downstream of the *Renilla* luciferase gene. In the same plasmid, the firefly luciferase gene was included as an internal control (Supplementary Figure S1). The result of the reporter assays indicated that the induction of *Cdx1* in SW480 cells caused a 38.9% (with an S.D. of 1.8) reduction in luciferase activity, indicating that *Cdx1* suppresses *CDX2* mRNA expression through the 3'UTR of these transcripts.

**Table 1** Fold induction of *Cdx2*-targeting miRNA candidates after *Cdx1* introduction

Quantitative RT-PCR analysis of miRNAs extracted from SW480 cells transduced with *Cdx1* for 6 days. Quantifications of miRNA expression changes are shown as relative values to the mock-transduced sample.

miRNA	Expression change	
	Microarray*	Quantitative RT-PCR*
<i>miR-9</i>	+ †	1.58
<i>miR-15a</i>	1.22	1.97
<i>miR-15b</i>	1.52	2.18
<i>miR-16</i>	1.38	2.02
<i>miR-22</i>	3.20	7.99
<i>miR-24</i>	0.80	1.11
<i>miR-103</i>	1.20	N/A
<i>miR-107</i>	1.29	1.74
<i>miR-181a</i>	8.29	8.82
<i>miR-181b</i>	8.93	14.04
<i>miR-181c</i>	Undetected	N/A
<i>miR-181d</i>	0.45	N/A
<i>miR-195</i>	Undetected	N/A
<i>miR-211</i>	Undetected	N/A
<i>miR-204</i>	Undetected	0.89
<i>miR-214</i>	Undetected	N/A

\*Ratio of a specific miRNA between the values before and after *Cdx1* introduction.

†Detectable only when *Cdx1* was exogenously expressed.

***miR-9*, *miR-16* and *miR-22* suppress *CDX2* mRNA by targeting of the 3'UTR**

To induce the exogenous expression of each of our candidate miRNAs, we prepared retrovirus vectors that express the corresponding pre-miRNA from the U6 promoter via RNA polymerase III. We next constructed reporter vectors containing



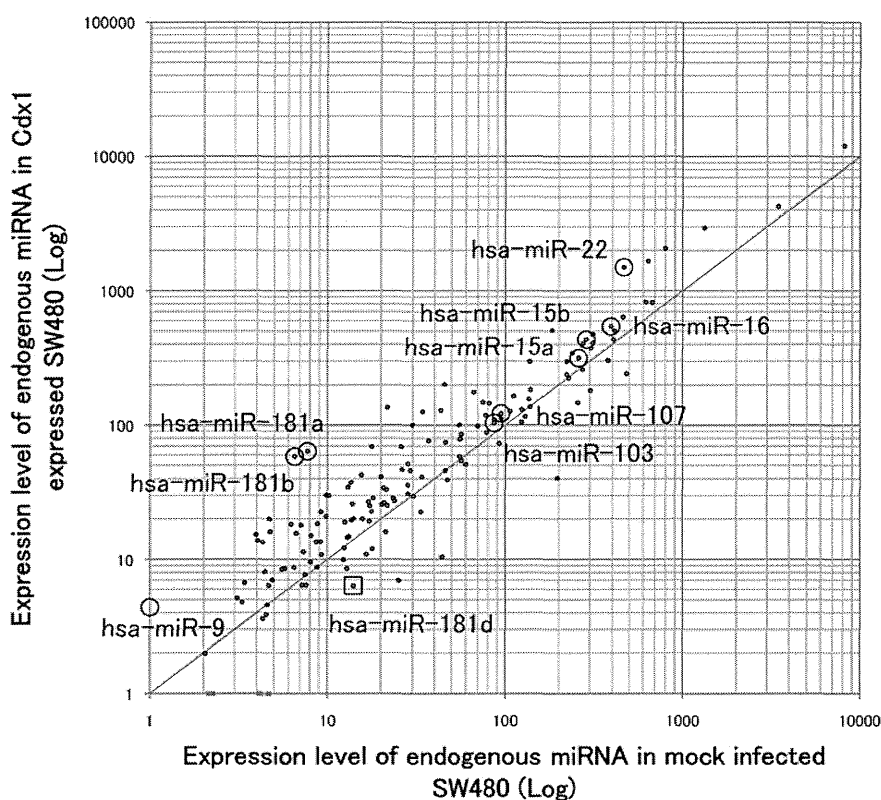


**Figure 3** Screening of miRNAs induced by Cdx1 transduction

Microarray analysis of miRNAs extracted from SW480 cells transduced with Cdx1 for 5 days. Black points show single miRNA species detected by microarray. miRNAs predicted to directly target *CDX2* mRNAs that are either up-regulated or down-regulated by exogenous Cdx1 expression are shown by circles (○) and rectangles (□), together with their names. The black diagonal line indicates the area where expression levels of miRNA have no difference in SW480 cells with or without exogenous Cdx1 expression. The expression level is shown as a log scale.

either a wild-type or mutated 3'UTR of *CDX2* mRNA cloned from the HCT116 cell line. We mutated the putative miRNA-binding sites so that the seed sequences of the known human miRNAs targeting this region would not match (Figure 2). The results of co-transfection experiments using miRNAs and these reporter vectors into SW480 cells indicated that *miR-9*, *miR-16* and *miR-22* could suppress luciferase activity (Figure 4A), whereas *miR-107* and *miR-181b* failed to do so (results not shown). Interestingly, it has been previously reported that, in gastric cancer cells, *miR-9* down-regulates *Cdx2* expression [17].

Importantly, *miR-16* and *miR-22* did not suppress reporter activity for the mutant vectors, indicating that these miRNAs suppress *CDX2* by directly binding to the 3'UTR of its transcripts. Interestingly, however, the luciferase activity levels of the reporter vector harbouring mutant *miR-9*-binding sites was not fully released from suppression by exogenous *miR-9*. This suppression was completely suppressed only when both the *miR-9*- and *miR-16*-binding sites were mutated (Figure 4A). Since exogenous *miR-9* expression did not significantly alter the endogenous *miR-16* levels (Supplementary Figure S4 at <http://www.BiochemJ.org/bj/447/bj4470449add.htm>), we speculate from this finding that *miR-9* might also affect *miR-16*-binding sites indirectly by regulating RNA-binding proteins that are associated with *CDX2* mRNA.

Importantly in this regard, the transfection of any of these three miRNAs to SW480 cells resulted in the down-regulation of endogenous *CDX2* mRNA (Figure 4B). Overall, these results indicate that *miR-9*, *miR-16* and *miR-22* are induced by exogenous Cdx1 expression and target *CDX2* mRNA to reduce its levels

through the direct binding of its 3'UTR, as well as through some additional mechanisms.

#### ***miR-9*, *miR-16* and *miR-22* play a critical role in suppressing Cdx2 through exogenous Cdx1 expression**

To finally understand the significance of *miR-9*, *miR-16* and *miR-22* during *Cdx2* suppression by exogenous Cdx1, we performed reporter assays in SW480 cells transduced with *CDX1* retrovirus vector or with an empty vector. Reporters having only mutations in the binding sites for *miR-9*, *miR-16* or *miR-22* failed to recover from the suppression by Cdx1. We found, however, that the mutations in both *miR-9*- and *miR-16*-binding sites led to an almost full recovery of luciferase activity from suppression by Cdx1 (Figure 5). Our observations that simultaneous mutations of both the *miR-9*- and *miR-16*-binding sites in the 3'UTR of *CDX2* mRNA blocks Cdx2 suppression indicate the critical roles of these miRNAs in this regulatory event of this colorectal tumour cell line.

#### **DISCUSSION**

In the present study, we hypothesized that, in colorectal cells, Cdx1 expression suppresses Cdx2 expression through the activity of some miRNAs. To test this possibility, we first identified several miRNAs which are induced by exogenous Cdx1 expression using high-throughput screening (Figure 3 and Table 1). Among the induced miRNAs we identified, we found that *miR-9*, *miR-16*

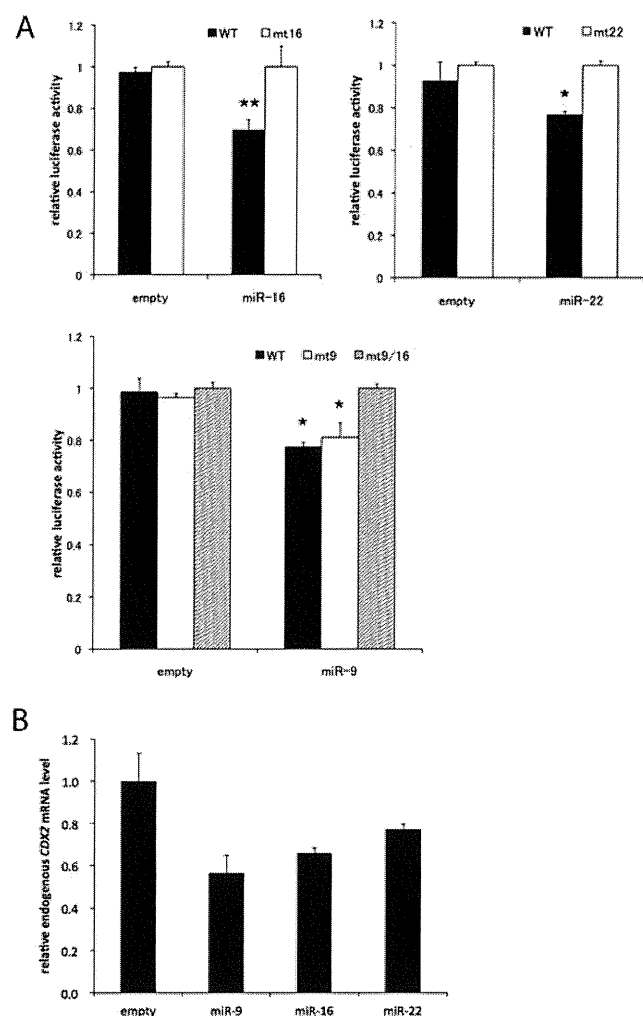


**Figure 4** Analysis of the suppressive ability of miRNAs through their binding to the *CDX2* mRNA 3'UTR

(A) SW480 cells were co-transfected with either psiCHECK-2-*Cdx2*\_3'UTR or mutant reporters, and miRNA expression vectors as indicated in the Figure. Dual luciferase assays were performed 48 h after transfection. \**P* < 0.05 and \*\**P* < 0.01 compared with the corresponding mock-transfected control. (B) Quantitative RT-PCR analysis of *CDX2* mRNA extracted from 1 × 10<sup>5</sup> SW480 cells which were transfected with 100 ng of empty vector or miRNA expression vectors as indicated in the Figure. RNA samples were extracted at 48 h post-transfection. \**P* < 0.05 and \*\**P* < 0.01 compared with the corresponding mock-transfected control. WT, wild-type.

and *miR-22* can efficiently target the 3'UTR of *CDX2* mRNA (Figure 4A). The miRNA-binding sites were pin-pointed within the 3'UTR; two were identified for each of the three miRNAs. Since simultaneous mutation of the two sites for *miR-9* is not sufficient for full recovery from the suppression by exogenous *miR-9* introduction, we speculated that there may be some other *miR-9*-binding sites and/or some other indirect suppression mechanisms that involve these sites (Figure 4A). We further confirmed that the exogenous expression of each of these miRNAs reduces the levels of the endogenous *CDX2* mRNA (Figure 4B).

There are two human *miR-16* gene loci (*miR-16-1* and *miR-16-2*) which simultaneously produce *miR-15a* and *miR-15b* respectively, both of which are elevated by the exogenous introduction of *Cdx1* (Table 1), i.e. both loci are *Cdx1*-responsive. Since *miR-16*, *miR-15a* and *miR-15b* share the same seed sequence, we anticipate that *miR-15a* and *miR-15b* may also

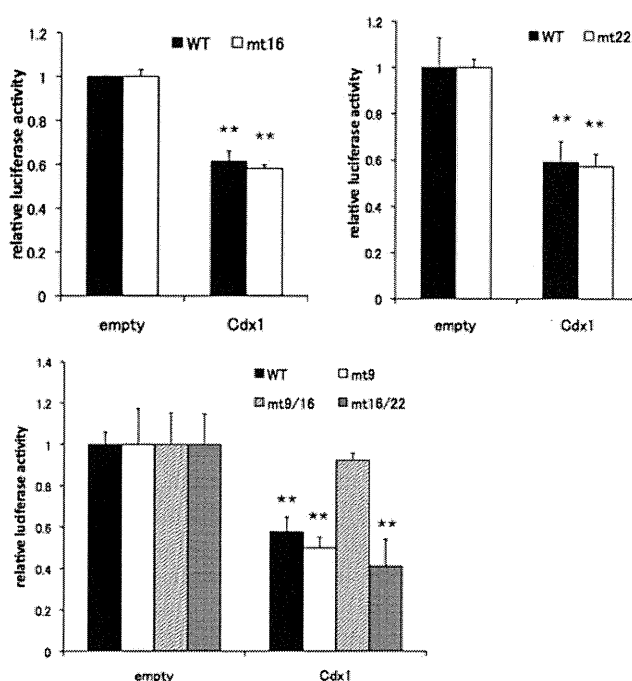


**Figure 5** *miR-9* and *miR-16* play an important role during the suppression of *CDX2* by *Cdx1* which occurs via the 3'UTR of *CDX2* transcripts

SW480 cells were transfected with *Cdx1* for 4 days and transfected with psiCHECK-2-*Cdx2*\_3'UTR or mutated reporter vectors as indicated. A dual luciferase assay was carried out 48 h post-transfection. \*\**P* < 0.01 compared with the mock-infected control. WT, wild-type.

contribute to the *Cdx1* suppression of *Cdx2*. Interestingly, it has been reported that *Cdx2* is down-regulated by phosphorylation via CDK2 (cyclin-dependent kinase 2) leading to its degradation following polyubiquitination [2,18]. However, since the results of the present study indicate that *Cdx1* represses *CDX2* mRNA and protein to similar extents, we think that *Cdx2* suppression is mainly caused by a direct function of *Cdx1*-inducible miRNAs.

We then evaluated how mutations within the identified binding sites for *miR-9*, *miR-16* or *miR-22* respectively, would effect reporters carrying the 3'UTR of *CDX2* in *Cdx1*-introduced cells (Figure 5). Interestingly, mutations in any one of these miRNA-binding sites alone did not cause a release from the suppression by *Cdx1*. This result is consistent with the idea that multiple miRNAs that target the same mRNA would often co-operate to achieve significant suppression. In this respect, the fact that the simultaneous mutations on both *miR-9*- and *miR-16*-binding sites almost fully cancelled out *Cdx2* suppression is a notable finding. It suggests that there are very critical roles for these two miRNAs in *Cdx2* suppression, at least in this colorectal cell line. Importantly, the *miR-22* gene is also *Cdx1*-responsive (Table 1 and Figure 3), and *miR-22* clearly targets *CDX2* mRNA (Figure 4). Therefore we believe *miR-22* would also play crucial roles in *Cdx2* suppression in many intestinal cells.

In summary, we have successfully identified a robust regulatory mechanism and some key factors involved in *Cdx2* suppression by *Cdx1*, which would at least partly explain the mutually exclusive expression patterns for these proteins reported in the intestinal epithelia of mice. This regulatory network formed by miRNAs themselves reveals the importance of homeostasis and the control of the transcriptional regulatory system through the limiting of transcription factors that share DNA recognition sequences. It has been proposed that miRNA fine-tunes regulatory networks

[19] and we have previously reported that miRNAs can also function as molecular switches forming double-negative feedback loops [20,21]. Therefore the results of the present study reveal a novel dimension of miRNA function which regulates expression levels among family members of the coding genes. By this regulatory mechanism, the levels of either Cdx1 or Cdx2 would be carefully regulated to establish and maintain stable gradients of their expression along the anterior–posterior axis of the gut [1]. This further suggests that Cdx1 and Cdx2 have distinct functions in the intestinal epithelium. To resolve the apparent functional differences between Cdx1 and Cdx2, further analyses both *in vitro* and *in vivo* (human and mouse intestinal epithelium), e.g. *in situ* hybridization of miRNA that we have developed [21,22] and immunohistochemical staining of Cdxs are needed.

#### AUTHOR CONTRIBUTION

Takanobu Tagawa carried out most of the experiments. pmU6-miR-16-1 was constructed by Takeshi Haraguchi. Hiroaki Hiramatsu and Kazuyoshi Kobayashi performed Western blotting and RT-PCR respectively after preparing high-titre retrovirus vectors. Ken-ichi Inada prepared the anti-Cdx1 antibody (rabbit). Takeshi Haraguchi, Kouhei Sakurai, Ken-ichi Inada and Hideo Iba provided technical support and advice. Takanobu Tagawa and Hideo Iba wrote the paper.

#### ACKNOWLEDGEMENTS

We thank S. Kawaura and A. Kato for assistance in the preparation of this paper. We thank J. Chang for the English editing before submission.

#### FUNDING

This work was supported by a Grant-in-Aid for Scientific Research on Priority Areas from the Ministry of Education, Culture, Sports, Science and Technology, Japan (MEXT) [grant number 17016015].

#### REFERENCES

- Guo, R.-J., Suh, E. R. and Lynch, J. P. (2004) The role of Cdx proteins in intestinal development and cancer. *Cancer Biol. Ther.* **3**, 593–601
- Coskun, M., Troelsen, J. T. and Nielsen, O. H. (2011) The role of CDX2 in intestinal homeostasis and inflammation. *Biochim. Biophys. Acta* **1812**, 283–289
- Hinoi, T., Lucas, P. C., Kuick, R., Hanash, S., Cho, K. R. and Fearon, E. R. (2002) CDX2 regulates liver intestine-cadherin expression in normal and malignant colon epithelium and intestinal metaplasia. *Gastroenterology* **123**, 1565–1577
- Margalit, Y., Yarus, S., Shapira, E., Gruenbaum, Y. and Fainsod, A. (1993) Isolation and characterization of target sequences of the chicken CdxA homeobox gene. *Nucleic Acids Res.* **21**, 4915–4922
- Savory, J. G. A., Pilon, N., Grainger, S., Sylvestre, J.-R., B eland, M., Houle, M., Oh, K. and Lohnes, D. (2009) Cdx1 and Cdx2 are functionally equivalent in vertebral patterning. *Dev. Biol.* **330**, 114–122
- Mutoh, H., Hayakawa, H., Sakamoto, H., Sashikawa, M. and Sugano, K. (2009) Transgenic Cdx2 induces endogenous Cdx1 in intestinal metaplasia of Cdx2-transgenic mouse stomach. *FEBS J.* **276**, 5821–5831
- Saegusa, M., Hashimura, M., Kuwata, T., Hamano, M., Wani, Y. and Okayasu, I. (2007) A functional role of Cdx2 in  $\beta$ -catenin signaling during transdifferentiation in endometrial carcinomas. *Carcinogenesis* **28**, 1885–1892
- Bonhomme, C., Calon, A., Martin, E., Robine, S., Neuville, A., Kedinger, M., Domon-Dell, C., Duluc, I. and Freund, J.-N. (2008) Cdx1, a dispensable homeobox gene for gut development with limited effect in intestinal cancer. *Oncogene* **27**, 4497–4502
- Crissey, M. A. S., Guo, R.-J., Fogt, F., Li, H., Katz, J. P., Silberg, D. G., Suh, E. R. and Lynch, J. P. (2008) The homeodomain transcription factor Cdx1 does not behave as an oncogene in normal mouse intestine. *Neoplasia* **10**, 8–19
- Yamamichi, N., Inada, K.-i., Furukawa, C., Sakurai, K., Tando, T., Ishizaka, A., Haraguchi, T., Mizutani, T., Fujishiro, M., Shimomura, R. et al. (2009) Cdx2 and the Brm-type SWI/SNF complex cooperatively regulate villin expression in gastrointestinal cells. *Exp. Cell Res.* **315**, 1779–1789
- Bartel, D. P. (2004) MicroRNAs: genomics, biogenesis, mechanism, and function. *Cell* **116**, 281–297
- Ambros, V. (2004) The functions of animal microRNAs. *Nature* **431**, 350–355
- Bartel, D. P. (2009) MicroRNAs: target recognition and regulatory functions. *Cell* **136**, 215–233
- Kozomara, A. and Griffiths-Jones, S. (2011) miRBase: integrating microRNA annotation and deep-sequencing data. *Nucleic Acids Res.* **39**, D152–D157
- Yu, J.-Y., DeRuiter, S. L. and Turner, D. L. (2002) RNA interference by expression of short-interfering RNAs and hairpin RNAs in mammalian cells. *Proc. Natl. Acad. Sci. U.S.A.* **99**, 6047–6052
- Benahmed, F., Gross, I., Guenet, D., Jehan, F., Martin, E., Domon-Dell, C., Brabletz, T., Kedinger, M., Freund, J. and Duluc, I. (2007) The microenvironment controls CDX2 homeobox gene expression in colorectal cancer cells. *Am. J. Pathol.* **170**, 733–744
- Gross, I., Lhermitte, B., Domon-Dell, C., Duluc, I., Martin, E., Gaiddon, C., Kedinger, M. and Freund, J.-N. (2005) Phosphorylation of the homeotic tumor suppressor Cdx2 mediates its ubiquitin-dependent proteasome degradation. *Oncogene* **24**, 7955–7963
- Rotkrue, P., Akiyama, Y., Hashimoto, Y., Otsubo, T. and Yuasa, Y. (2011) MiR-9 downregulates CDX2 expression in gastric cancer cells. *Int. J. Cancer* **129**, 2611–2620
- Sevignani, C., Calin, G. A., Siracusa, L. D. and Croce, C. M. (2006) Mammalian microRNAs: a small world for fine-tuning gene expression. *Mamm. Genome* **17**, 189–202
- Fujita, S., Ito, T., Mizutani, T., Minoguchi, S., Yamamichi, N., Sakurai, K. and Iba, H. (2008) miR-21 gene expression triggered by AP-1 is sustained through a double-negative feedback mechanism. *J. Mol. Biol.* **378**, 492–504
- Sakurai, K., Furukawa, C., Haraguchi, T., Inada, K.-i., Shiogama, K., Tagawa, T., Fujita, S., Ueno, Y., Ogata, A., Ito, M. et al. (2010) microRNAs miR-199a-5p and -3p target the Brm subunit of SWI/SNF to generate a double-negative feedback loop in a variety of human cancers. *Cancer Res.* **71**, 1680–1689
- Yamamichi, N., Shimomura, R., Inada, K.-i., Sakurai, K., Haraguchi, T., Ozaki, Y., Fujita, S., Mizutani, T., Furukawa, C., Fujishiro, M. et al. (2009) Locked nucleic acid *in situ* hybridization analysis of miR-21 expression during colorectal cancer development. *Clin. Cancer Res.* **15**, 4009–4016

Received 12 March 2012/10 July 2012; accepted 31 July 2012

Published as BJ Immediate Publication 31 July 2012, doi:10.1042/BJJ20120434

**SUPPLEMENTARY ONLINE DATA**

**Multiple microRNAs induced by Cdx1 suppress Cdx2 in human colorectal tumour cells**

Takanobu TAGAWA\*, Takeshi HARAGUCHI\*, Hiroaki HIRAMATSU\*, Kazuyoshi KOBAYASHI\*, Kouhei SAKURAI\*, Ken-Ichi INADA† and Hideo IBA\*<sup>1</sup>

\*Division of Host–Parasite Interaction, Department of Microbiology and Immunology, Institute of Medical Science, University of Tokyo, 4-6-1 Shirokanedai, Minato-ku Tokyo 108-8639, Japan, and †First Department of Pathology, Fujita Health University School of Medicine, Aichi, Japan

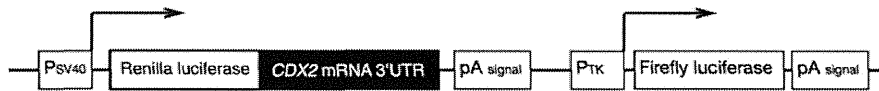


**Figure S1 Model of luciferase reporter plasmid**

The luciferase reporter plasmid contains *CDX2* mRNA 3'UTR downstream of the *Renilla* luciferase coding sequence. Firefly luciferase worked as the inner control.

5' ...UAGAAAGCUGGACUGACCAAGA... (WT)	5' ...UUGUGUUGUUGUUGCUGCUG... (WT)
3' AGUAUGUCGAUCUAUUGGUUCU (miR-9)	3' GCGGUUAAAUGCAGCAGAU (miR-16)
XXXX:X	XXXX:X
5' ...UAGAAAGCUGGACUGCGCGGA... (mt9-1)	5' ...UUGUGUUGUUGUUGCGGUUG... (mt16-2)
5' ...UUUAGAGAGCCUGUCACCAGAGC... (WT)	5' ...CUGCGGAAGCCAAAGGCAGCUA... (WT)
:	
3' AGUAUGUCGAUCUAUUGGUUCU (miR-9)	3' UGUCAAGAAGUUGACCGUCGAA (miR-22-2)
XXXXX:X	XXXX :X
5' ...UUUAGAGAGCCUGCCGUAGCC... (mt9-2)	5' ...CUGCGGAAGCCAAAUCCGUAA... (mt22-2)
3' UGUCAAGAAGUUGACCGUCGAA (miR-22)	5' ...AGAGCUUCUCUGGGCUGAUGUUAU... (WT)
X	
5' ...CUUGAGGCCAAGAUGGCUGCUGC... (WT)	3' UGAGUGGCUGCGCAACUUACAA (miR-181a)
	x xx x
3' GCGGUUAAAUGCAGCAGAU (miR-16)	5' ...AGAGCUUCUCUGGGCUUAUAGCUU... (mt181)
XX X:X	
5' ...CUUGAGGCCAAGAUGCGUAUCGC... (mt16-1/22-1)	
XXXXX:X	
3' UGUCAAGAAGUUGACCGUCGAA (miR-22)	

| Watson-Crick pair  
 : non Watson-Crick pair  
 X no pairing  
 Underline mutated position

**Figure S2 miRNA-binding sites and mutations within the 3'UTR of *CDX2* mRNA**

Sequence of the putative binding sites of *miR-9*, *miR-16*, *miR-22* and *miR-181*. Mutations used in the luciferase assay are also indicated. WT, wild-type.

<sup>1</sup> To whom correspondence should be addressed (email iba@ims.u-tokyo.ac.jp).

<p>Position 36-42 of CDX2 3' UTR            hsa-miR-24            5' ...CAGAGCAAUCCAGGCUGAGCCA...                                                               3'     GACAAGGACGACUUGACUCGGU</p>	<p>Position 498-504 of CDX2 3' UTR            hsa-miR-22            5' ...ACUGCGGAGCCAAAGGCAGCUA...                                                               3'     UGUCAAGAAGUUGACCGUCGAA</p>
<p>Position 343-353 of CDX2 3' UTR            hsa-miR-103            5' ...CUUCCUAGAUCUGCAG-GCUGACCUC...                                                               3'     AGUAUCGGGACAUGUUACGACGA</p>	<p>Position 524-531 of CDX2 3' UTR            hsa-miR-9            5' ...UAGAAAGCUGGACUGACCAAGA...                                                               3'     AGUAUGUCGAUCUAU-UGGUUUCU</p>
<p>Position 387-394 of CDX2 3' UTR            hsa-miR-204            5' ...GGGAGAGAGGGACUC-AAGGGAAA...                                                                      3'     UCCGUAUCCUACUGUUUCCCUU</p>	<p>Position 690-696 of CDX2 3' UTR            hsa-miR-9            5' ...UUAGAGAGCCUGUCACCAGACUUC...                                                               3'     AGUAUGUCGAUCUAUUGGUUUCU</p>
<p>Position 403-410 of CDX2 3' UTR            hsa-miR-24            5' ...AAGGGAAAGGCAAGCUUGAGGCCAA...                                                               3'     GACAAGGACGACUUGACUC-GGU</p>	<p>Position 708-714 of CDX2 3' UTR            hsa-miR-181a            5' ...AGAGCUUCUCUGGGCUGAAUGUA...                                                               3'     UGAGUGGCUGUCGCAACUUACAA</p>
<p>Position 414-421 of CDX2 3' UTR            hsa-miR-22            5' ...GCUUGAGGCCAAGAUGGCUGCUGCC...                                                               3'     UGUCAAGAAGUUGACCGUCGAA</p>	<p>Position 814-820 of CDX2 3' UTR            hsa-miR-16            5' ...AGUUUGUGUUGUUGUUGCUGCUG...                                                               3'     GCGGUUUAUAAUUGCAGCAGCAU</p>
<p>Position 416-421 of CDX2 3' UTR            hsa-miR-103            5' ...AAGCUUGAGGCCAAGAUGGCUGCUGCC...                                                               3'     AGUAUCGGGACAUGUUACGACGA</p>	<p>Position 814-820 of CDX2 3' UTR            hsa-miR-103            5' ...GGAGUUUGUGUUGUUGUUGCUGCUG...                                                               3'     AGUAUCGGGACAUGUUACGACGA</p>
<p>Position 416-421 of CDX2 3' UTR            hsa-miR-16            5' ...CUUGAGGCCAAGAUGGCUGCUGCC...                                                               3'     GCGGUUUAUAAUUGCAGCAGCAU</p>	<p>Position 816-822 of CDX2 3' UTR            hsa-miR-214            5' ...AGUUUGUGUUGUUGUUGCUGCUGUUUGG...                                                               3'     UGACGGACAGACACGGACGACA</p>
<p>Position 417-422 of CDX2 3' UTR            hsa-miR-214            5' ...UUGAGGCCAAGAUGGCUGCUGCCUGCU...                                                               3'     UGACGGACAGACACGGACGACA</p>	<p>Position 902-908 of CDX2 3' UTR            hsa-miR-204            5' ...AGAAGUGAUUGGUGAAGGGAA...                                                               3'     UCCGUAUCCUACUGUUUCCCUU</p>

**Figure S3** Sequences of predicted miRNA target sites in the *CDX2* mRNA 3'UTR shown in Figure 2 of the main text

Data was extracted from PicTar or TargetScan (restricted to targets which are 'broadly conserved among vertebrates'). Predicted nucleotides positions in the 3'UTR where the seed of miRNAs bind to are also indicated.

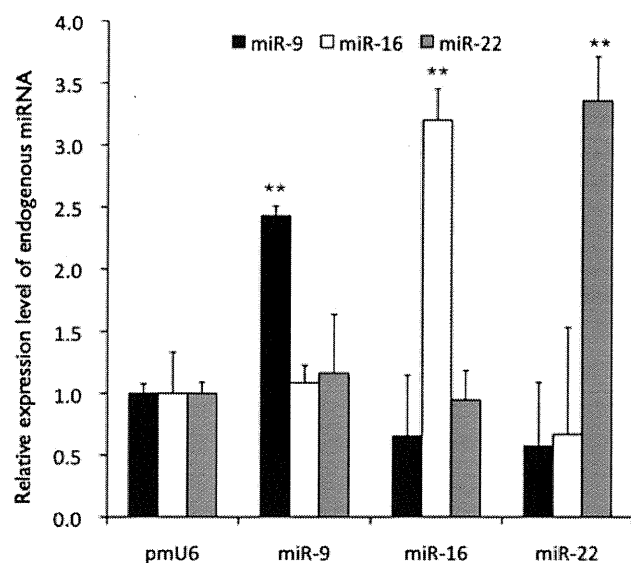


**Figure S4** Quantitative RT-PCR analysis of induced miRNAs in SW480 cells

miRNAs were extracted from SW480 cells which were transfected with empty vector or miRNA expression vectors as indicated in the Figure. Samples were extracted at 48 h post-transfection. \*\* $P < 0.01$  compared with the mock-infected control.

**Table S1** Sequence of synthetic deoxyoligonucleotides used in the present study

Underlining indicates the recognition sequences of restriction enzymes indicated in the Experimental section of the main text.

Purpose	Name	Sequence (5' → 3')	Antisense
Molecular cloning	<i>CDX2</i> mRNA 3'UTR	TCTAGACCACCGGGTTTCGACGCGGC	GGCCGGCCATCTGGAAAGCTCATTATCTC
Site-directed mutagenesis of psiCHECK-2-Cdx2_3'UTR	<i>miR-9</i> site 1	GGTTCTGCAGTCGCGCCGAGTCCAGC	GCTGGACTGCGGCGCAGTGCAGAACC
	<i>miR-9</i> site 2	CCAGAGAAGGCTACCGGACAGGCTCTC	GAGAGCCTGTCCGGTAGCCTTCTCTGG
	<i>miR-16</i> site 1/ <i>miR-22</i> site1	GGCCAAGATGCGTATCGCCTGCTCATGG	CCATGAGCAGGCGATACGCATCTTGGCC
	<i>miR-16</i> site 2	GTGTTGTTGTCGGTTTCGTTGGTTGTTG	CAACAACCCAAACGAACCGAACAAACAC
	<i>miR-22</i> site 2	CCAGCTTTCTATCTTACGCGATTGGCTTCCGCAGTG	CACTGCGGAAGCCAATCGCGTAAAGATAGAAAGCTGG
	<i>miR-181</i> site	CACCAGAGCTTCTCTGGGCTTATAGCTTGCAGTGCAT AAATGC	GCATTATAGCACTGACAAGCTATAAGCCAGAGAAGCT CTGGTG
miRNA expression vector	<i>miR-9-3</i>	<u>GAAGACTGTTTGAGCACGTGGAGCCACGGCGCGGCAG</u> CGGCACTGGCTAAGGGAGGCCGTTTCTCTCTTTG GTTATCTAGCTGATGAGTGCCACAGAGCCGTCA	<u>GAATTCGGGGCGGTGCGTGGGGCGGCGCTCGCACG</u> CAGAAGTTGTGAGAATCATTCTACTTTCCGGT TATCTAGCTTTATGACGGCTCTGTGGCACTCA
	<i>miR-16-1</i>	TTTGTTGTTCTCCATCAGATGTTGTTGCATGTTGGATG AACTGACATACTTGTCCACTTAGCAGCA CGTAAATATTGGCGTAGTGAATATATATAAACACC	AAAAAAGGGAAATACAACAATTGATCTAATAGTTGCTGT ATCCCTGTCACACTAAAGCAGCAGATAATATT GGTGTTAATATATATTTCACTACG
	<i>miR-22</i>	<u>GAAGACCAATTGGGCTGAGCCGACAGTTCCTCAGTGGC</u> AAGCTTTATGTCCTGACCCAGC	<u>GAATTCGGCAGAGGGCAACAGTTCTTCAACTGGCAGCT</u> TTAGCTGGGTCAGGACATAAAGC
	<i>miR-107</i>	<u>GAAGACCAATTGCTCTCTGCTTTCAGTTCCTTACAGTGT</u> GCCTTGTGGCATGGAGTTC	<u>GAATTCCTGTGCTTTGATAGCCCTGTACAATGCTGCTTG</u> AACTCCATGCCACAAGGCA
	<i>miR-181b-2</i>	<u>GAAGACCAATTGCTGATGGCTGCACTCAACATTCATTGCT</u> GTCGGTGGGTTGAGTCTGAATCAAC	<u>GAATTCGTTTGGTCCGACAGTTTGCATTCATTGATCAGTG</u> AGTTGATTCAGACTCAAACCC
	Quantitative RT-PCR	<i>CDX1</i> mRNA	GCCGACGCCCTACGAGTGGAA
<i>CDX2</i> mRNA		GAACCTGTGCCGAGTGGATG	GGATGGTGATGTAGCGACTG
<i>GAPDH</i>		CTCTGCTCCTCTGTTCCGAC	TAAAAGCAGCCCTGGTGAC

Received 12 March 2012/10 July 2012; accepted 31 July 2012

Published as BJ Immediate Publication 31 July 2012, doi:10.1042/BJ20120434